Electronic Supplementary Information

Development of potent tripodal G-quadruplex DNA binders and the efficient delivery to cancer cells by aptamer functionalised liposomes

Isabel Pont,[a] Cristina Galiana-Roselló,[a] Maria Sabater-Arcis,[b] Ariana Bargiela,[c] Juan Carlos Frias,[d] M. Teresa Albelda,[a] Jorge González-García,[a] Enrique García-España[a]

[a] Instituto de Ciencia Molecular (ICMol), Departamento de Química Inorgánica. Universidad de Valencia. C/. Catedrático José Beltrán 2, 46980, Paterna, Spain

[b] Translational Genomics Group, Incliva Health Research Institute, Valencia, Spain. Interdisciplinary Research Structure for Biotechnology and Biomedicine (ERI BIOTECMED), University of Valencia, Valencia, Spain. CIPF-INCLIVA Joint Unit, Valencia, Spain.

[c] Neuromuscular Research Unit, Neurology Department, Hospital La Fe, Instituto de Investigación Sanitaria La Fe (IISLAFE), Valencia.

[d] Department of Biomedical Science, CEU Cardenal Herrera University, Ramón y Cajal s/n, 46115 Alfara del Patriarca, Spain

Table of Contents

1.- Experimental Procedures

General Procedures. Mass spectrometry, NMR and elemental experiments were performed at the *Central Service for Experimental Science* (SCSIE) of the University of Valencia. Deuterated solvents for NMR purposes were obtained from Sigma-Aldrich and used as received. ^{1}H NMR and ^{13}C NMR were recorded on a Bruker Advance 300 spectrometer operating at 300 MHz (^{1}H) and 75.4 MHz (^{13}C). ^{1}H and ^{13}C chemical shifts (δ) were referenced internally to solvent shift and to internal standard TMS (D_2O: ^{1}H δ: 1.94, ^{13}C δ: 118.7; Acetone-d_6: ^{1}H δ:2.05, ^{13}C δ: 29.7). Chemical shifts are quoted in ppm, the downfield direction being defined as positive. The following abbreviations are used for convenience in reporting the multiplicity of NMR resonances: s, singlet; d, doublet; t, triplet; q, quartet; m, multiplet. All NMR data was acquired and processed using Topspin and MestreNova software respectively. Mass spectrometry analysis was performed under either ESI^+ condition on a LCT Premier mass spectrometer. UV Vis absorption spectra were recorded on a Varian Cary 100 Bio spectrophotometer and fluorescence emission spectra on a PTI spectrofluorimeter using a microcuvette with *l* =1 cm.

Chemical and reagents. All reagents were obtained from commercial sources and used without further purification. The phospholipidic molecules were purchased from Avanti Polar Lipids (USA) or NOF (Japan). The dialysis membrane (Spectra/Por®6 Dyalisis, MWCO: 2000 Da) was provided by Fisher. The DNA oligonucleotides were purchased from IDT (Integrated DNA Technologies, Belgium) in HPLC purity grade.

Synthesis of TPA-based compounds

The synthesis and characterisation of the TPA-based compounds been described previously in reference [1]. Briefly, the general method for the synthesis is the following. A solution of the corresponding mono-, di- or trialdehyde of the triphenylamine (1–2 mmol) dissolved in anhydrous ethanol (150 mL) was added dropwise to a solution of 1, 2 or 3 equivalents of the polyamine substituent dissolved in dry ethanol (50 mL). The mixture was stirred under nitrogen for 12 h at room temperature, resulting in the formation of the Schiff base. Reduction of the imines was performed by adding 10 equivalents of $NaBH_4$ and further stirring for 2 h. Then, the solvent was removed under reduced pressure. The resulting residue was treated with H_2O (20 mL) and extracted with CH_2Cl_2 (3 x 30 mL). The organic phase was dried over Na_2SO_4 and evaporated to afford a yellow oil, which was dissolved in anhydrous ethanol and precipitated with HCl in dioxane (0.4 M) to yield the hydrochloride salt of the product.

4-[10-Methyl-(2,6,10-undecaphan-1-yl)]triphenylamine (**TPA1P**): Yield: 53%; ^{1}H NMR (300 MHz, D_2O): δ=7.24 (d, *J*=9 Hz, 2H), 7.05–7.00 (m, 4H), 6.89–6.84 (m, 8H), 4.09 (s, 2 H), 3.32–3.27 (m, 2 H), 3.22– 3.14 (m, 6 H), 2.95 (s, 6 H), 2.26–2.14 ppm (m, 4H); ^{13}C NMR (75.2 MHz, D_2O): δ=149.1, 147.4, 131.5, 129.9, 125.1, 124.0, 123.1, 54.6, 51.2, 45.1, 44.9, 44.2, 43.2, 23.1, 21.7 ppm; ESI-MS: *m/z*: 417.0 $[M+H]^+$; elemental analysis calcd. (%) for $C_{27}H_{36}N_4 \cdot 3\ HCl \cdot H_2O$ (543.99 g/mol): C 59.6, H 7.6, N 10.3; found: C 60.2, H 8.3, N 11.7.

4,4'-Bis[10-methyl-(2,6,10-undecaphan-1-yl)]triphenylamine (**TPA2P**): Yield: 61%; ^{1}H NMR (300 MHz, D_2O): δ = 7.43–7.37 (m, 6H), 7.24–7.16 (m, 7H), 4.24 (s, 4 H), 3.33–3.18 (m, 16H), 2.95 (s, 12H), 2.26–2.13 ppm (m, 8H); ^{13}C NMR (75.2 MHz, D_2O): δ=148.9, 147.2, 131.6, 130.2, 126.0, 124.9, 124.1, 54.6, 51.1, 45.1, 44.9, 44.1, 43.2, 23.1, 21.6 ppm; ESI-MS: *m/z*: 588.3 $[M+H]^+$; elemental analysis calcd. (%) for $C_{36}H_{57}N_7 \cdot 6\ HCl$ (806.23 g/mol): C 50.8, H 13.9, N 11.2; found: C 53.6, H 7.9, N 12.1.

4,4',4''-Tris[10-methyl-(2,6,10-undecaphan-1-yl)]triphenylamine (**TPA3P**): Yield: 72%; ^{1}H NMR (300 MHz, D_2O): δ=7.45 (d, *J*=10 Hz, 6 H), 7.24 (d, *J*=9 Hz, 6 H), 4.27 (s, 6H), 3.33–3.20 (m, 24H), 2.95 (s, 18H), 2.28–2.13 ppm (m, 12 H); ^{13}C NMR (75.2 MHz, D_2O): δ=148.5, 131.7, 125.7, 125.0, 54.6, 51.2, 45.1, 44.9, 44.2, 43.2, 23.1, 21.6 ppm; ESI-MS: *m/z*: 759.53 $[M+H]^+$; elemental analysis calcd. (%) for $C_{45}H_{78}N_{10} \cdot 9HCl \cdot 8H_2O$ (1231.33 g/mol): C 43.9, H 8.4, N 11.4; found: C 45.7, H 10.9, N 11.6.

4-[({2-[3,6,9-triaza-1(2,6)-pyridinacyclodecaphan-6-yl]ethyl}amino)methyl]-N,N-diphenylaniline (**TPA1Py**): Yield: 23 %. ^{1}H NMR (300 MHz, D_2O): *δ*=7.92–7.87 (t, *J*=8 Hz, 1 H), 7.40–7.37 (d, *J*=8 Hz, 2 H), 7.23–7.20 (d, *J*=8 Hz, 2 H), 7.02–6.97 (t, *J*=15 Hz, 4 H), 6.84–6.81 (d, *J*=7 Hz, 8 H), 4.57 (s, 2 H), 4.08 (s, 2 H), 3–29-3.15 (m, 6 H), 3.04–2.96 (m, 2 H), 2.88–2.78 ppm (m, 4 H); ^{13}C NMR (75.4 MHz, D_2O): *δ*=149.20, 147.47, 140.17, 131.64, 129.92, 125.14, 124.08, 123.06, 122.56, 51.39, 50.83, 49.87, 46.29, 30.63 ppm; MS (ESI^+): *m*/*z* (%): 507.3 $[M+H]^+$; elemental analysis calcd (%) for $C_{32}H_{38}N_6 \cdot 3\ HCl \cdot 2.5\ H_2O$: C 58.17, H 7.02, N 12.72; found: C 57.97, H 7.53, N 12.66.

4-[({2-[3,6,9-triaza-1(2,6)-pyridinacyclodecaphan-6-yl]ethyl}amino)methyl]-N-{4-[({2-[3,6,9-triaza-1(2,6)-pyridinacyclodecaphan-6-yl]ethyl}amino)methyl]phenyl}-N-phenylaniline (**TPA2Py**): Yield: 47 %. ^{1}H NMR (300 MHz, D_2O): *δ*=8.03–7.98 (t, *J*=8 Hz, 2 H), 7.51–7.40 (m, 8 H), 7.27–7.19 (m, 7 H) 4.68 (s, 8 H), 4.29 (s, 4 H), 3.41–3.30 (m, 12 H), 3.16–3.10 (m, 4 H), 2.99–2.95 ppm (m, 8 H); ^{13}C NMR (75.4 MHz, D_2O): *δ*=151.79, 151.46, 149.75, 142.69, 134.15, 132.79, 128.61, 127.52, 126.63, 125.10, 54.00, 53.81, 53.41, 52.42, 48.84, 45.46 ppm; MS (ESI^+): *m*/*z* (%): 384.03 $[M+2H]^{2+}$; elemental analysis calcd (%) for $C_{46}H_{61}N_{11} \cdot 5\ HCl \cdot 6.7\ H_2O$: C 51.58, H 7.47, N 14.39; found: C 51.86, H 7.76, N 14.30.

Tris{4-[({2-[3,6,9-triaza-1(2,6)-pyridinacyclodecaphan-6-yl]ethyl}amino)methyl]phenyl}amine (**TPA3Py**): Yield: 22 %. ^{1}H NMR (300 MHz, D_2O): *δ*=7.98 (t, *J*=8 Hz, 3 H), 7.46 (m, 12 H), 7.22 (d, *J*=9 Hz, 6 H), 4.66 (s, 12 H), 4.28 (s, 6 H), 3.39 (m, 6 H), 3.30 (m, 12 H), 3.12 (m, 6 H), 2.96 ppm (t, *J*=5 Hz, 12 H); ^{13}C NMR (75.4 MHz, D_2O): *δ*=149.49, 148.76, 140.41, 131.94, 126.07, 125.21, 122.81, 51.73, 51.51, 51.12, 50.11, 46.54, 43.29 ppm; elemental analysis calcd (%) for $C_{60}H_{84}N_{16}\cdot 9\,HCl\cdot 11\,H_2O$: C 46.32, H 7.44, N 14.40; found: C 46.82; H 7.83; N, 14.01.

Encapsulation of TPA3P/TPA3Py/TPB3P/TPB3Py in liposome nanoparticles. The liposome nanoparticles including the TPA derivative were synthesized by lipid film hydration and further sonication in order to obtain unilamellar vesicles. Generally, the lipid composition was POPC, mPEG2000-DSPE and DPPE-NBD at molar ratio 80:3:2. In a typical synthesis, the lipids were dissolved in 5 mL of chloroform and then, the solvent was removed by rotary evaporation yielding a dry lipid film and further dried under vacuum overnight. The resulting film was hydrated by adding an aqueous solution of **TPA3P, TPA3Py, TPB3P or TPB3Py** hydrochloride salt at 75 °C. Particularly, for the targeted-liposomes functionalisation the aptamer AS1411 (300 µL of a 22 µM solution) was also included in the hydration step. The resulting suspension was sonicated using a probe tip sonicator and finally centrifuged (10 minutes at 3200 rpm). The non-encapsulated compound was removed from the liposome suspension by thorough dialysis in milliQ water during three days. The liposome suspension was stored at 4 °C to further studies.

Encapsulation Efficiency determination. The quantification of the encapsulated **TPA3P/TPA3Py/TPB3P/TPB3Py** was carried out by fluorescence spectroscopy accordingly to **TPA3P/TPA3Py/TPB3P/TPB3Py** standard curve. The spectra of **TPA3P/TPA3Py TPB3P/TPB3Py** increasing concentrations in MeOH:Water (90:10) were recorded upon excitation at 314 nm. The emission maxima were plotted against the **TPA3P/TPA3Py TPB3P/TPB3Py** concentration, obtaining a calibration curve by least-squares fitting. An aliquot of the liposome suspension under assessment was incubated 10 minutes in MeOH:Water (90:10) after through mixing, in order to disrupt the vesicles and release the cargo. Then, the emission spectrum of the sample was registered using the same conditions used in the standard measurements. The concentration of the encapsulated **TPA3P/TPA3Py TPB3P/TPB3Py** was calculated by interpolation in the calibration curve. The final obtained value and its associated error results from averaging three replicates.

Particle size characterization. Dynamic light scattering (DLS) was used in order to estimate the particle size distribution of the liposome suspensions. The measurements were carried out

in a Malvern Mastersizer 2000 equipment equilibrating the sample at 25 °C. Each experiment was performed in triplicate.

Cell Culture. MCF-7 and HeLa cells were kindly provided by the Cell Culture Section of the *Central Service for Experimental Science* (SCSIE) of the University of Valencia. LN229 cells were generously supplied by Dr. Priam Villalonga (University of the Balearic Islands, Spain). Dulbecco's Modified Eagle's Medium (DMEM) High Glucose, fetal bovine serum (FBS) penicillin and streptomycin were purchased from Thermo Fisher. Scientific. All cell lines were grown in DMEM, which was supplemented with 10% heat-inactivated FBS (30 min, 56 ºC), 100 U/mL penicillin and 10 µg/L streptomycin. The cultures were maintained at 37 ºC in a humidified environment with 5% CO_2. The growth and the proliferation of the cells were regularly checked using an optical microscope by assessment of the cell morphology, the adherent conditions and the absence of contamination.

Cell Viability Assays. Cell viability was determined with the 3-(4,5-dimethylthiazol-2-yl)-2,5-diphenyltetrazolium bromide (MTT) assay described previously. MTT is reduced by the mitochondrial reductase enzymes of living cells to give formazan crystals, which is directly related to the number of viable cells.[3] Briefly, cells were seeded (4000 cells per well) in 96-well flat bottom microplates with complete medium. After 24 hours, the medium was replaced by different ligand concentrations referring either to the free form, the encapsulated into the un-targeted liposomes or into the targeted-liposomes. Then, the plates were further exposed to 48 hours of incubation. At that point, 10 µL of a 12 mM MTT stock solution were added to each well and the plates were left to stand for 4 hours. Finally, 100 µL of DMSO were incorporated to each well in order to dissolve the formazan crystals. The absorbance at 570 nm was measured using an ESPECTRA-MAX PLUS microplate spectrophotometer. The data analysis and the IC_{50} calculation were performed with the software Origin2017 accordingly to non-linear curve fitting.

Confocal laser scanning microscopy. The evaluation of liposome cell uptake was carried out by using an Olympus FV1000MPE microscope. LN229 cells were plated in 65 mm plates (10000 cells per plate) and incubated in standard conditions for 24 hours allowing the cells to adhere. Then, the medium was replaced by 2 ml of medium containing different concentrations of both, targeted and un-targeted liposomes. In this case, liposomes do not include the ligands in order to avoid the cell death. After 24 hours of treatment, the medium was eliminated and the plates were washed with PBS, leaving finally 2 ml of PBS per well. The images were acquired exciting at 463 nm and the emission collected at 536 nm.

2.- Figures and tables

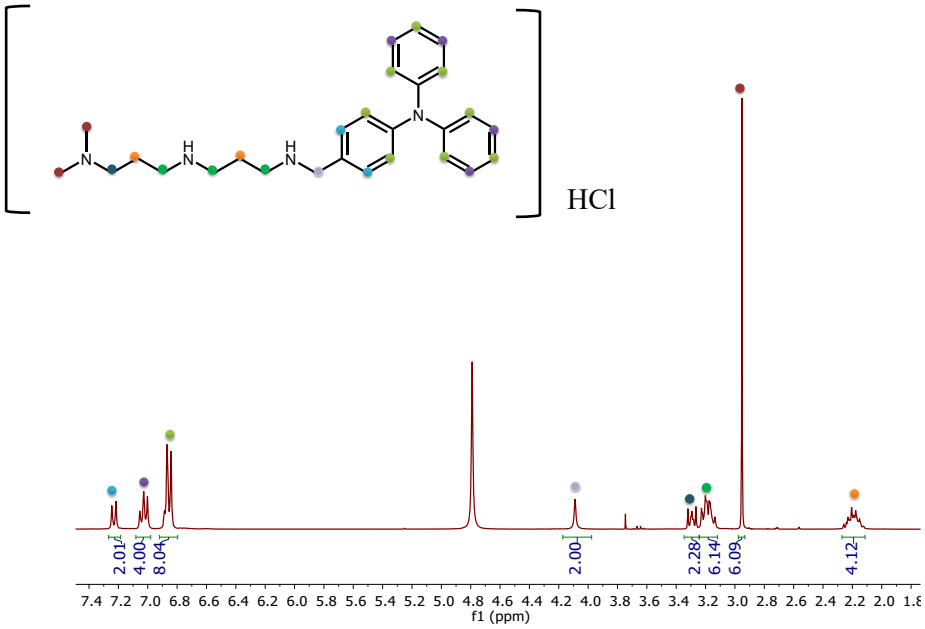

Figure S1.- ^{1}H-NMR and ^{13}C-NMR spectra of **TPA1P** hydrochloride salt in D_2O

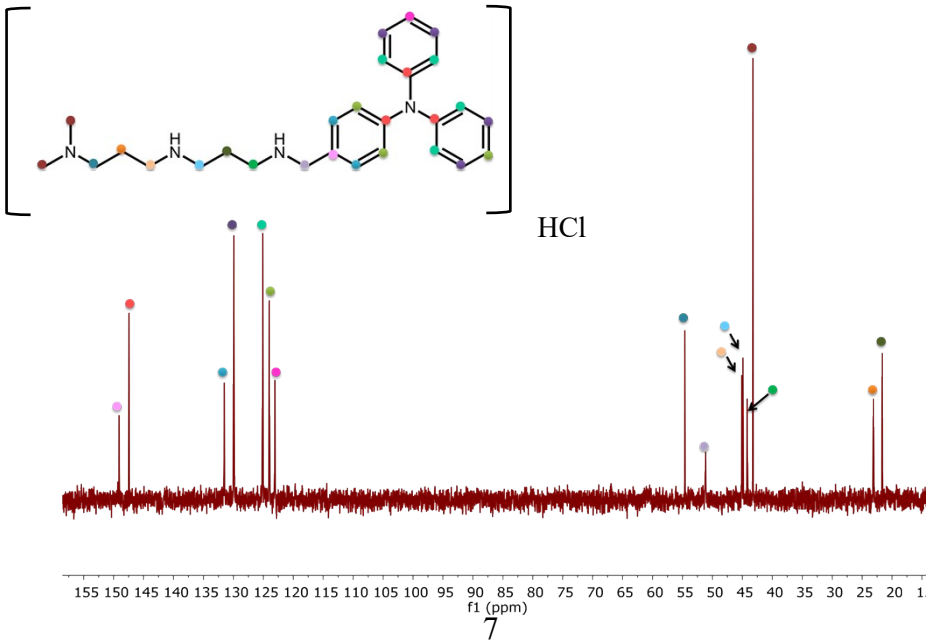

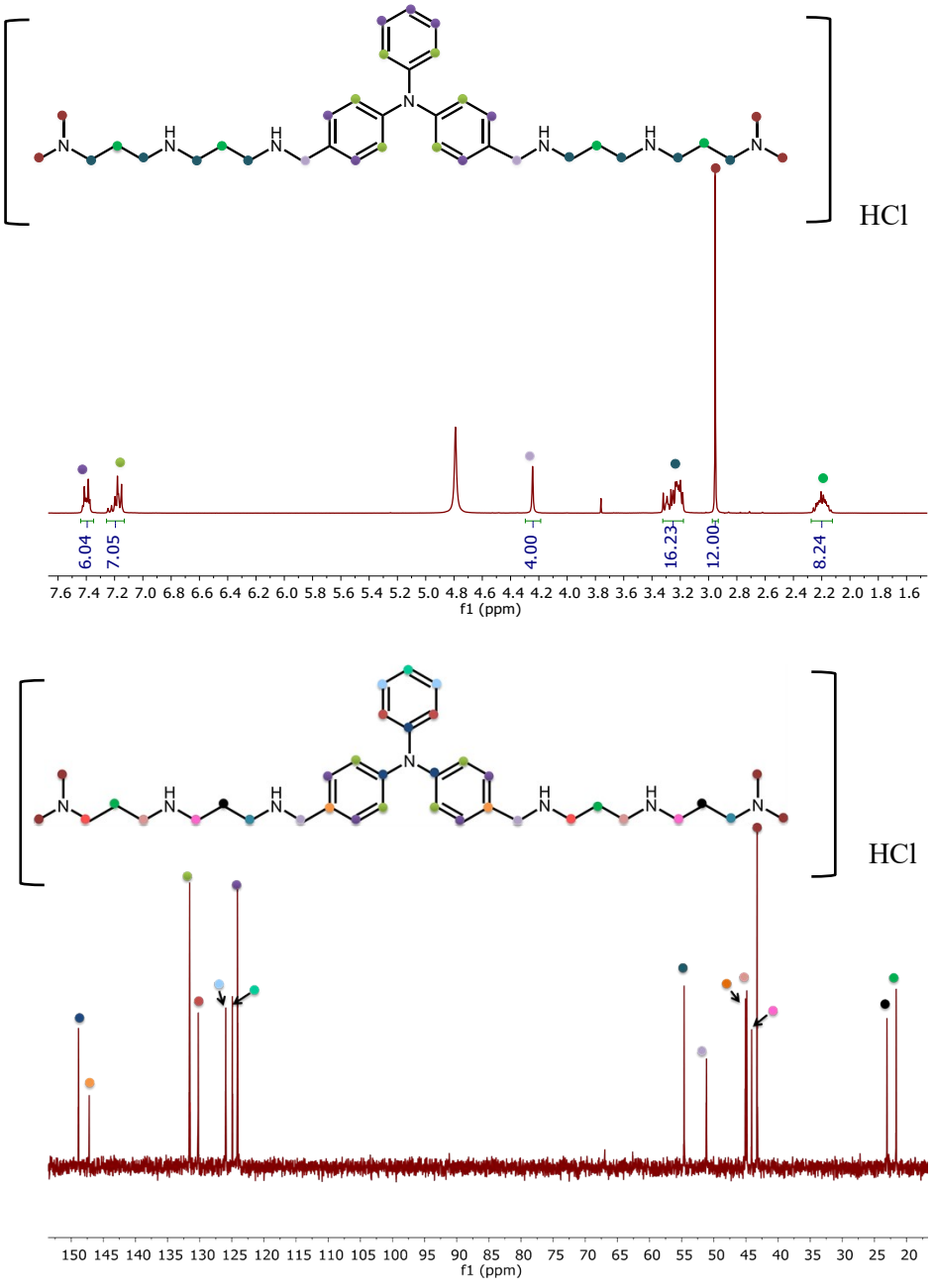

Figure S2.- ^{1}H-NMR and ^{13}C-NMR spectra of **TPA2P** hydrochloride salt in D_2O

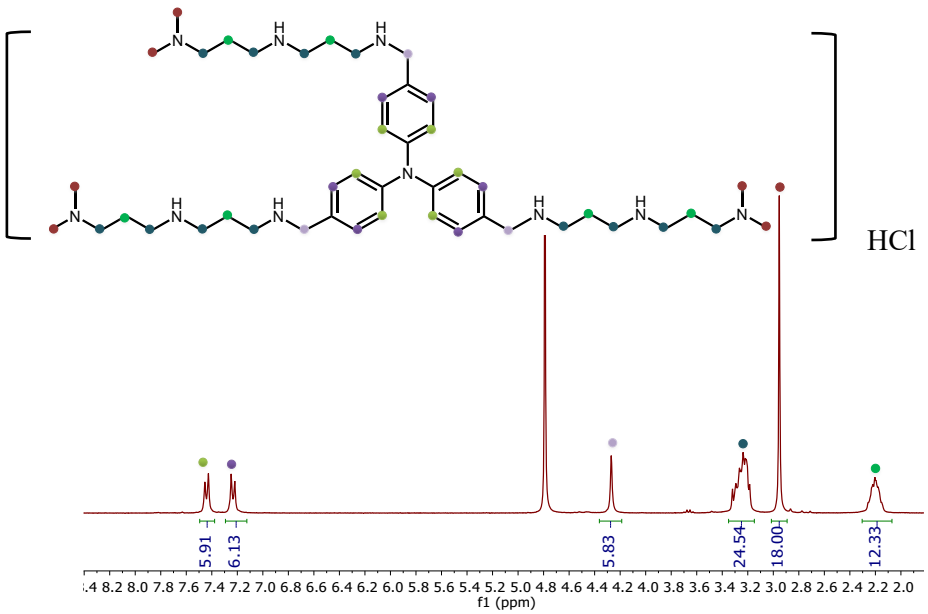

Figure S3.- ^{1}H-NMR and ^{13}C-NMR spectra of **TPA3P** hydrochloride salt in D_2O

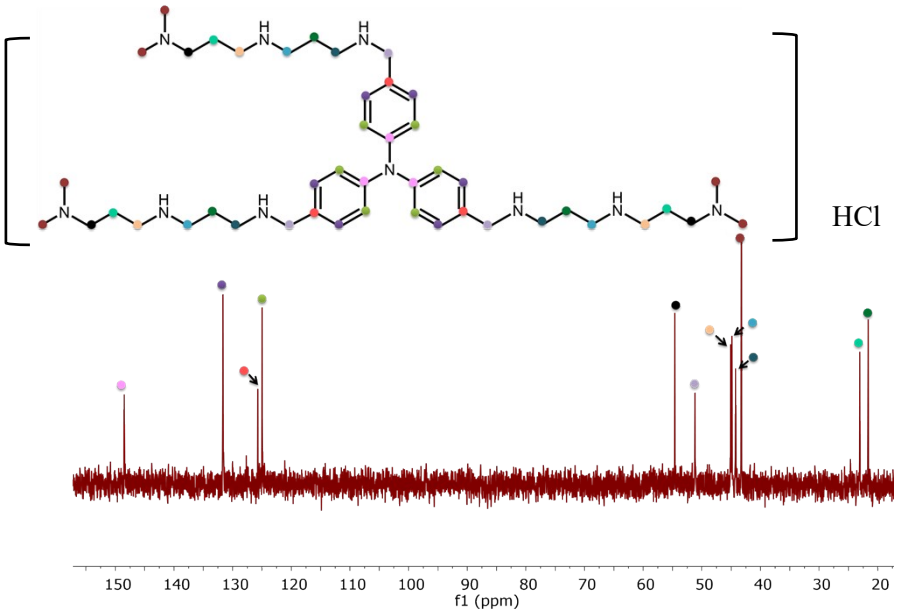

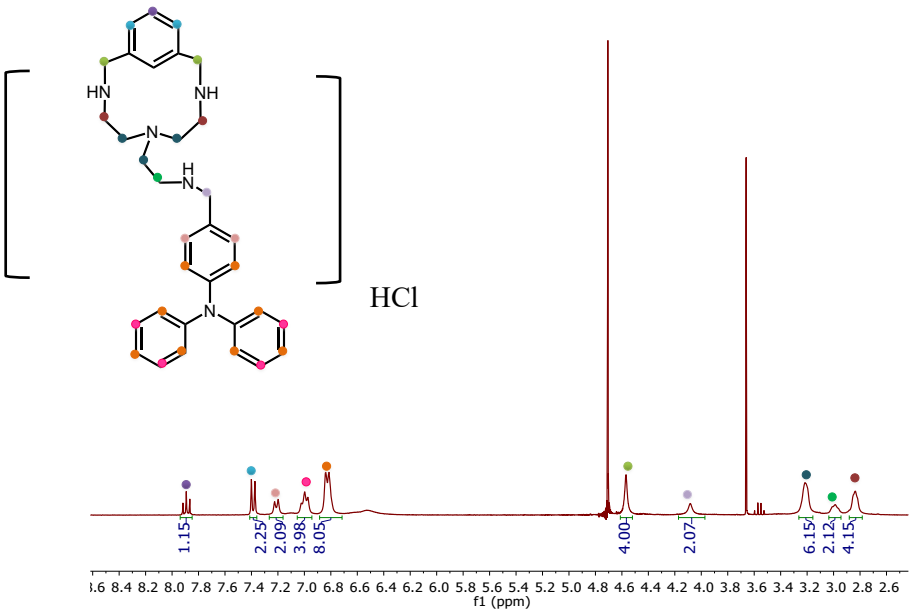

Figure S4.- ^{1}H-NMR and ^{13}C-NMR spectra of **TPA1Py** hydrochloride salt in D_2O

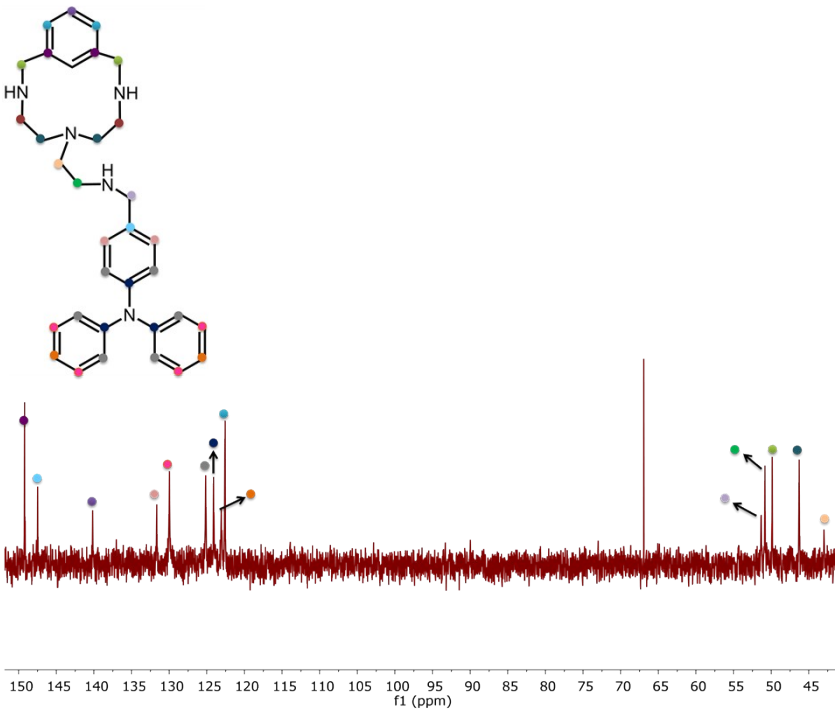

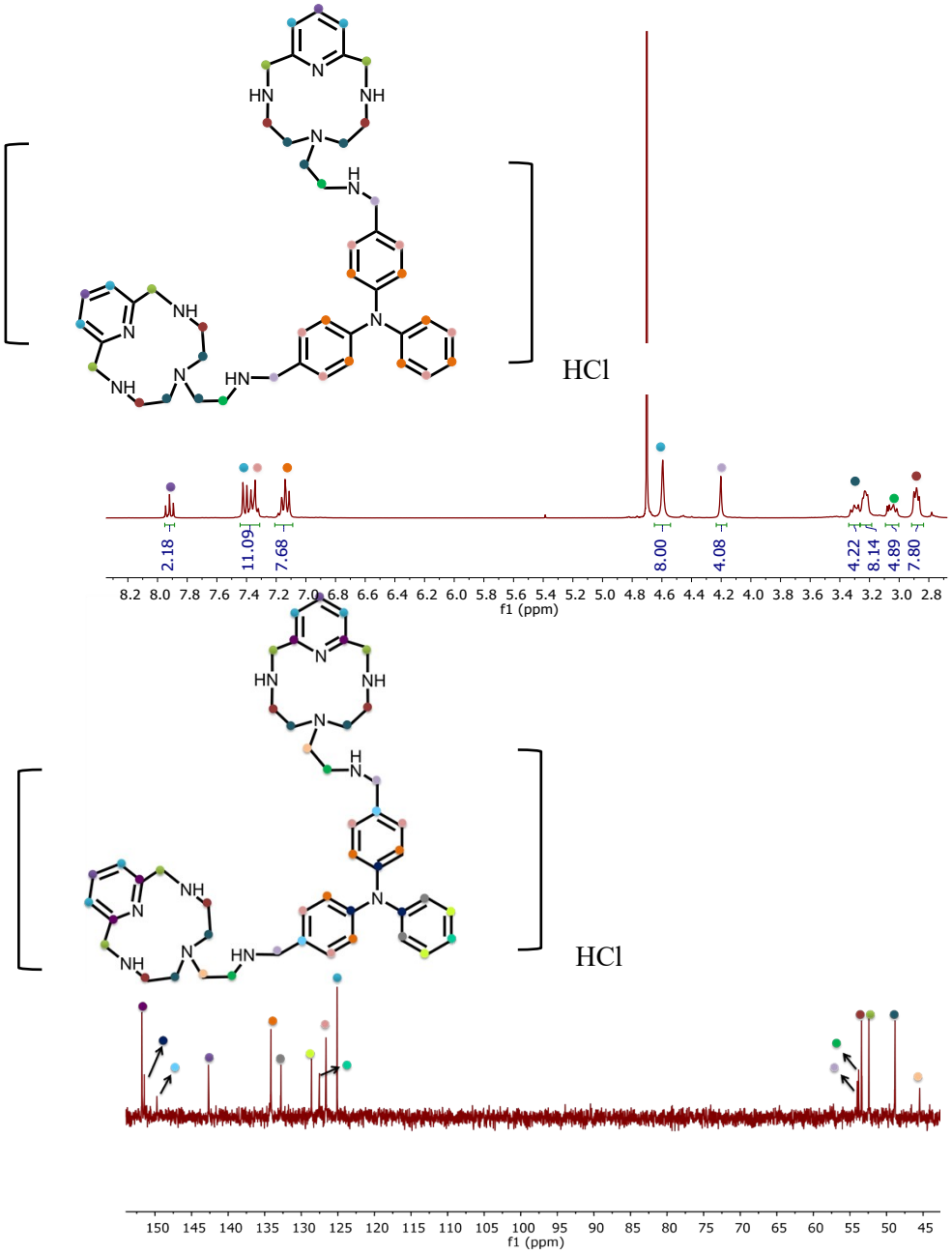

Figure S5.- ^{1}H-NMR and ^{13}C-NMR spectra of **TPA2Py** hydrochloride salt in D_2O

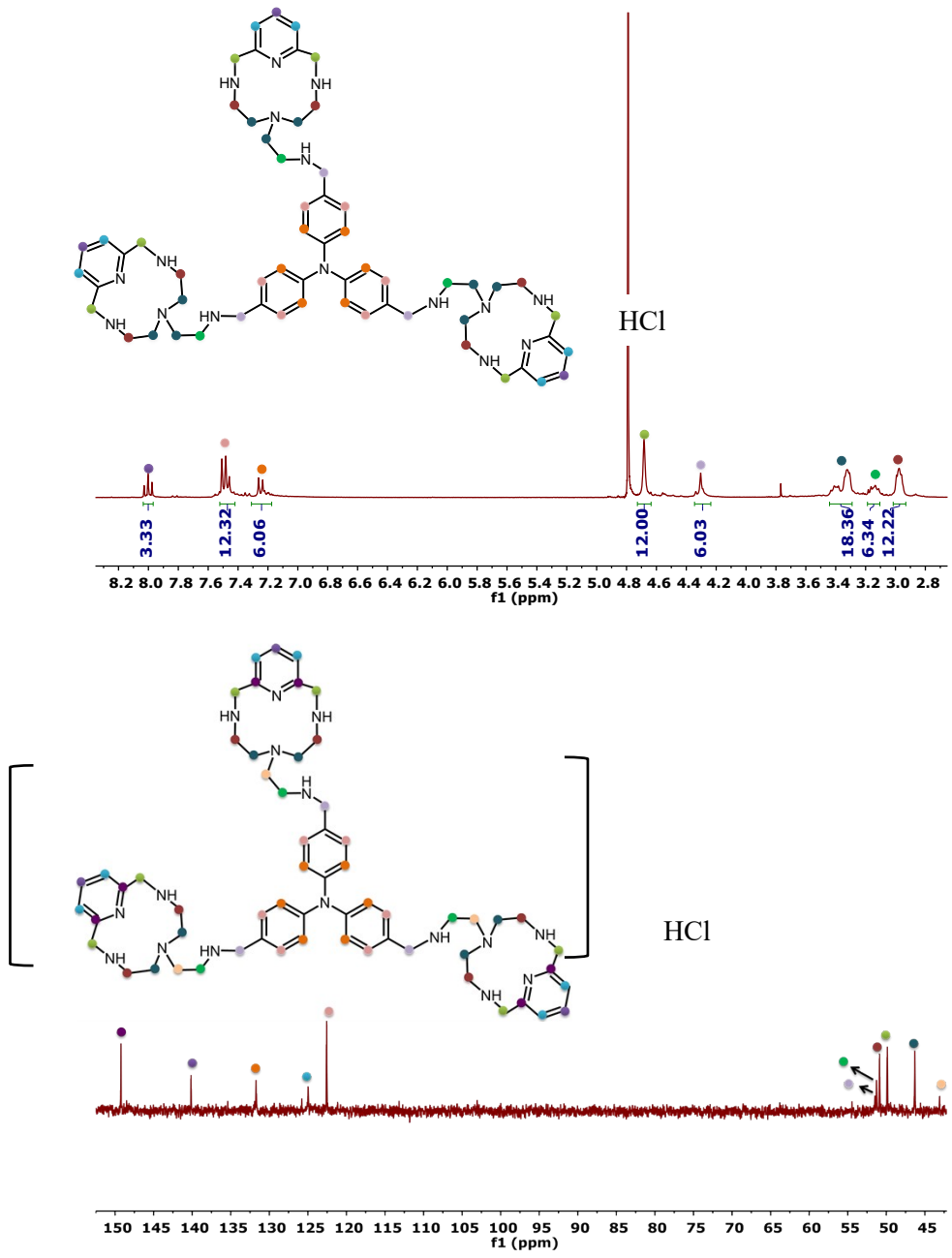

Figure S6.- ^{1}H-NMR and ^{13}C-NMR spectra of **TPA3Py** hydrochloride salt in D_2O

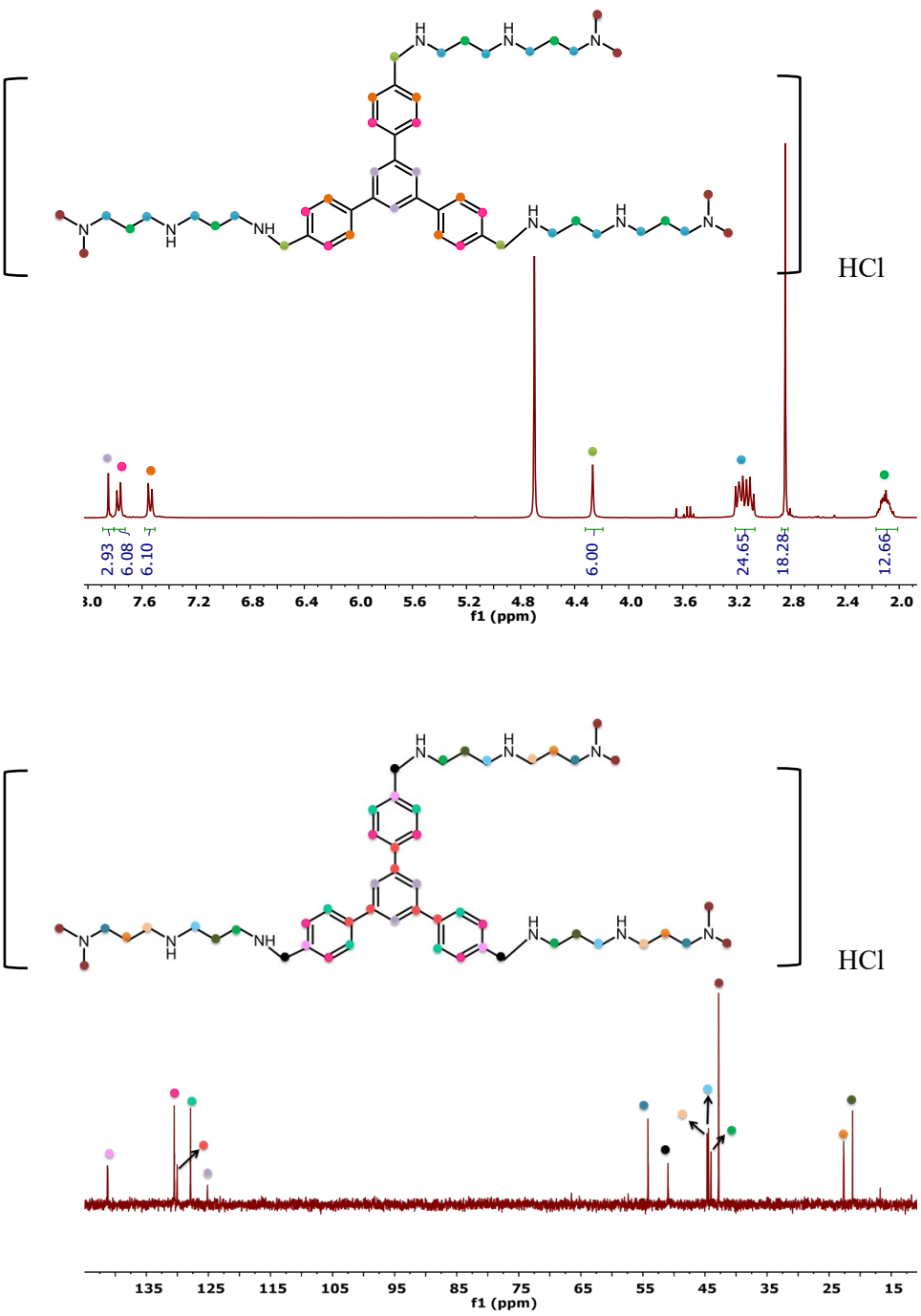

Figure S7.- ^{1}H-NMR and ^{13}C-NMR spectra of **TPB3P** hydrochloride salt in D_2O

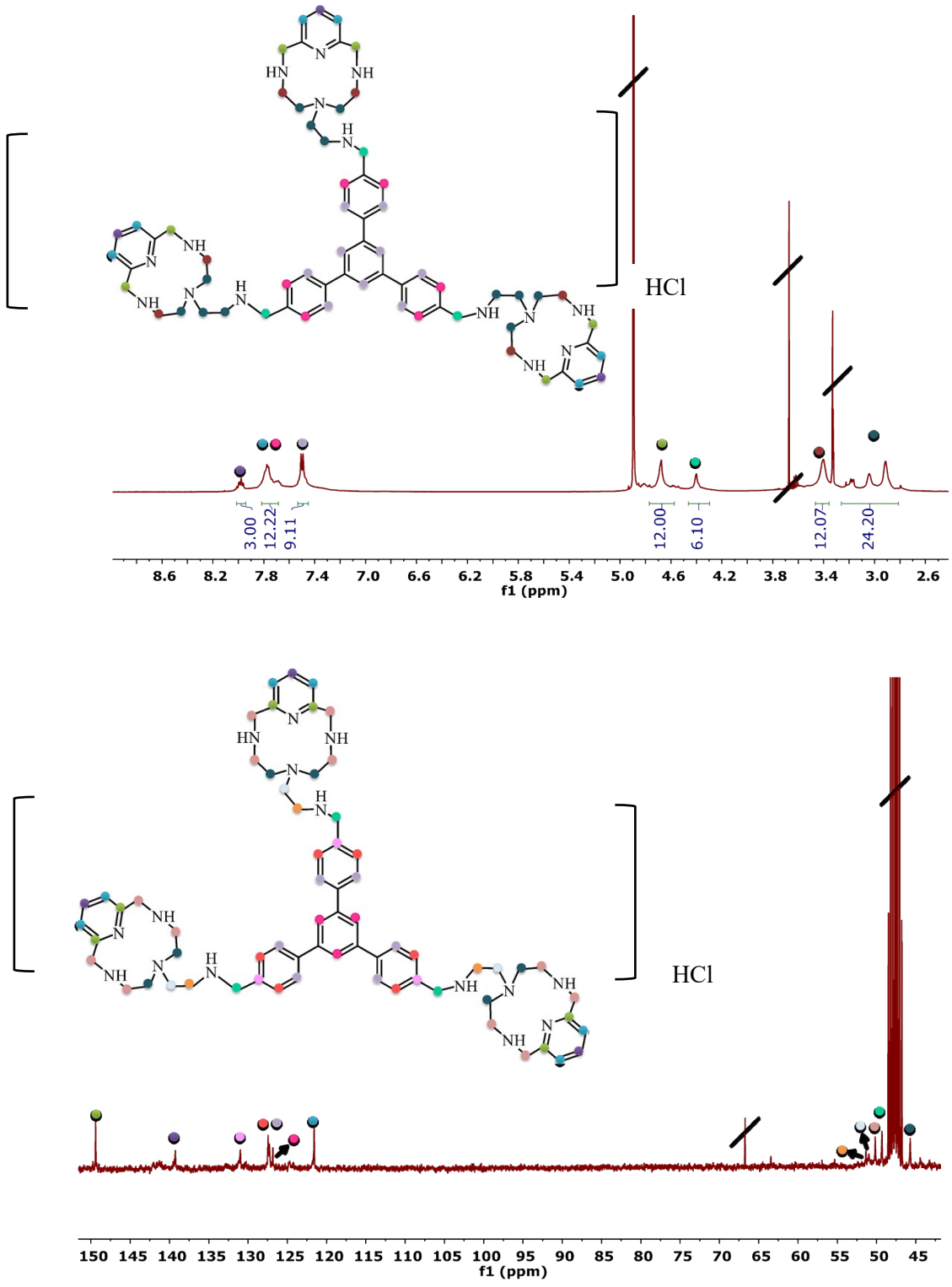

Figure S8.- ^{1}H-NMR and ^{13}C-NMR spectra of **TPB3Py** hydrochloride salt in D_2O

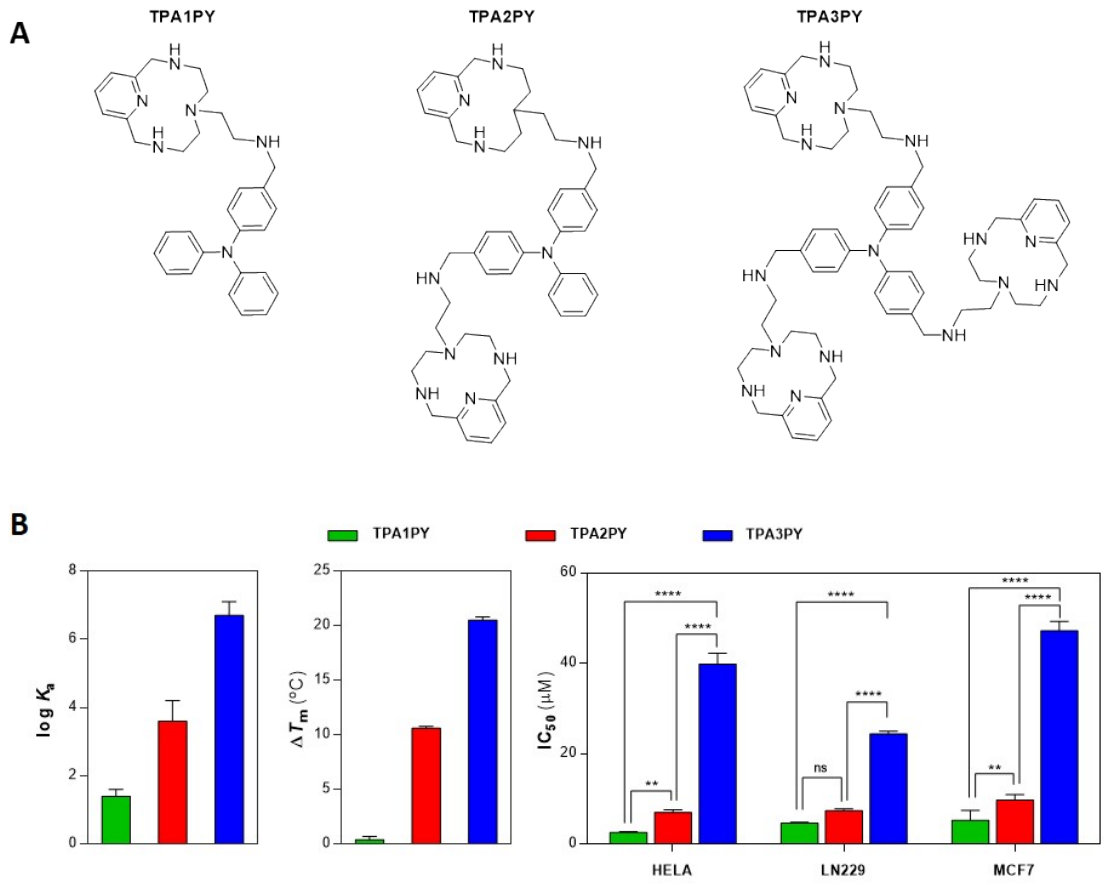

Figure S9. (A) Structures of TPA-Py based molecules under study. (B) Values of log K_a, ΔT_m (°C) and IC_{50} (μM) obtained from fluorimetric titrations, FRET melting and viability assays, respectively.

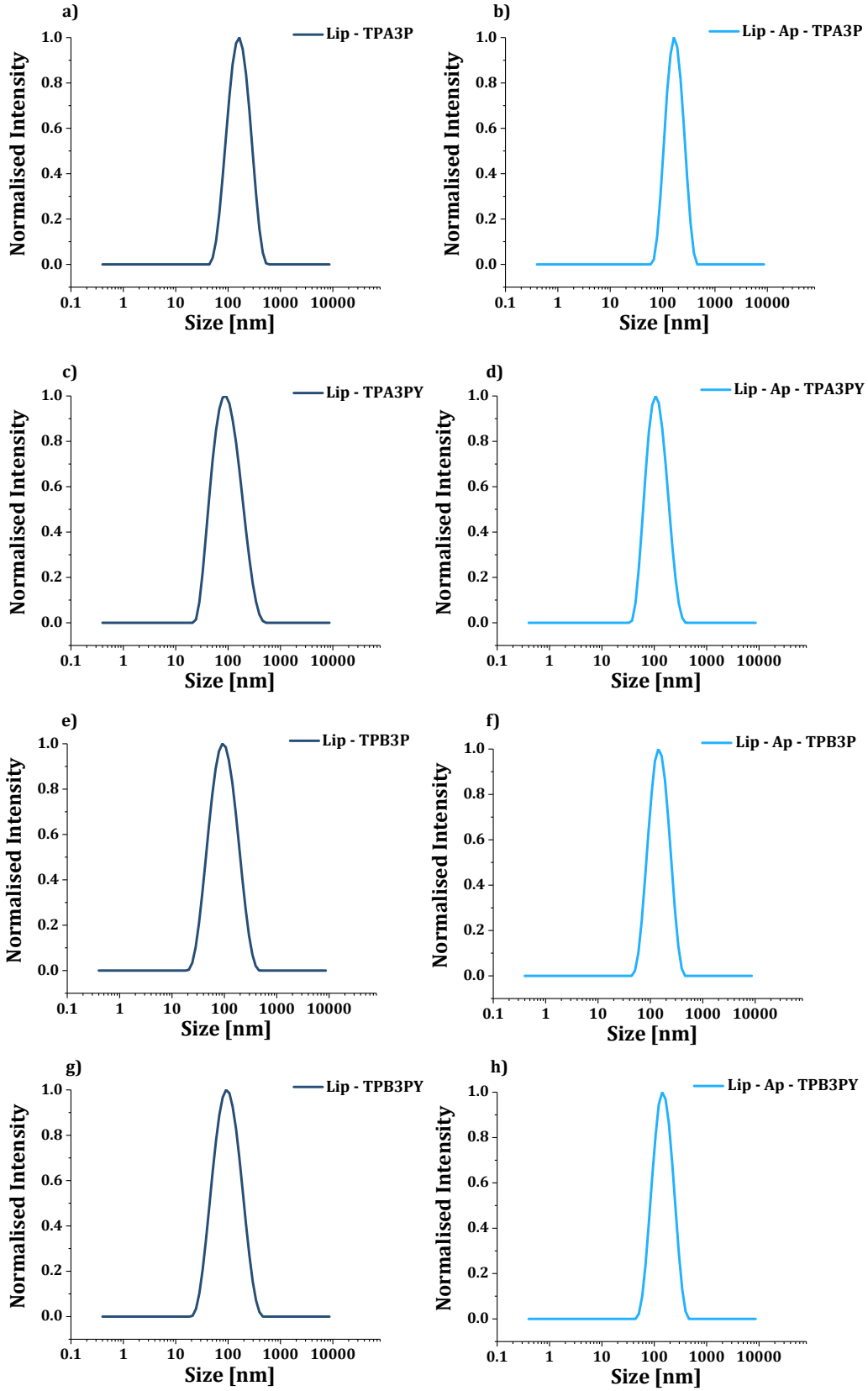

Figure S10. Average dynamic light scattering (DLS) spectra of liposome solutions under study.

Table S1. Average size of liposome formulations.[a]

Liposomes Formulation	Average size measured by DLS
TPA3P-Lip	134(4)
TPA3P-Lip+Apt	148(6)
TPA3Py-Lip	81(2)
TPA3Py-Lip+Apt	101(2)
TPB3P-Lip	82(3)
TPB3P-Lip+Apt	124(5)
TPB3Py-Lip	83(2)
TPB3Py-Lip+Apt	125(4)

[a] Values in parentheses are standard deviations in the last significant figure.

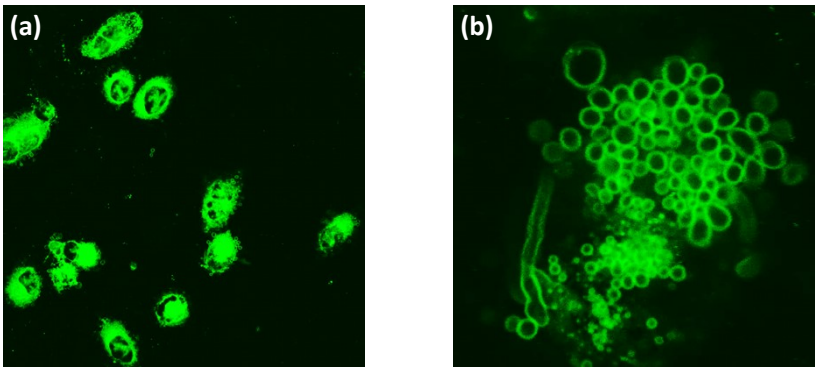

Figure S11. Image of confocal fluorescence microscopy of the liposomes in suspension.

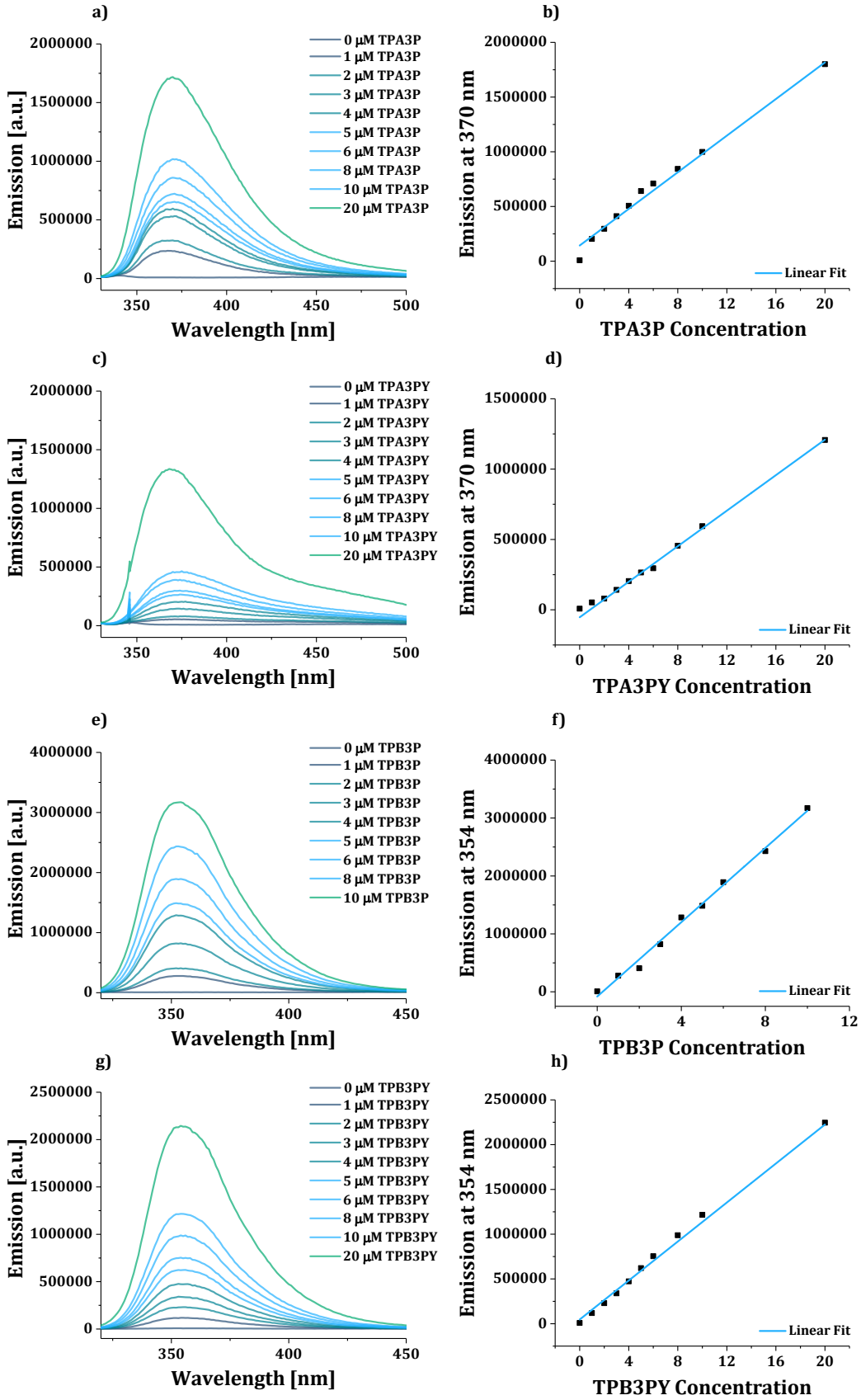

Figure S12. Emission spectra of increasing concentrations of ligand standards (right) and their corresponding standard curve (left).

Table S2. Quantification of the therapeutic component inside the synthesised liposomes.[a]

Liposomes Formulation	Concentration [μM]
TPA3P-Lip	424(2)
TPA3P-Lip+Apt	323(5)
TPA3Py-Lip	261(8)
TPA3Py-Lip+Apt	265(9)
TPB3P-Lip	72(1)
TPB3P-Lip+Apt	45(1)
TPB3Py-Lip	43.8(6)
TPB3Py-Lip+Apt	44(2)

[a] The emission was registered after disrupting the vesicles using a mixture MeOH/Water. All the measurements were performed at least in triplicate. Values in parentheses are standard deviations in the last significant figure.

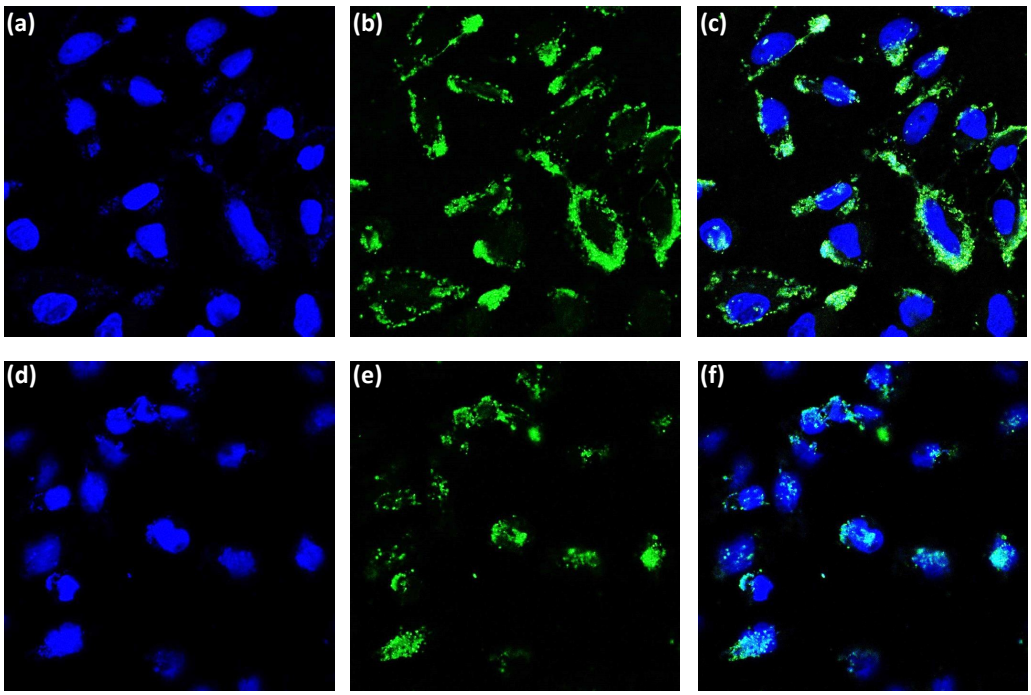

Figure S13.- Confocal microscopy images of live LN229 cells treated with **Lip** (a, b and c) and **Lip+Apt** (d, e and f). LN229 cells were treated with the liposomal formulations at 37°C for 1 hour, after which they were incubated with Hoechst 33342 at 37°C for 30 minutes. Blue nuclear stain, DAPI filter (a and d), green stain (b and e) and merge both channels (c and f).

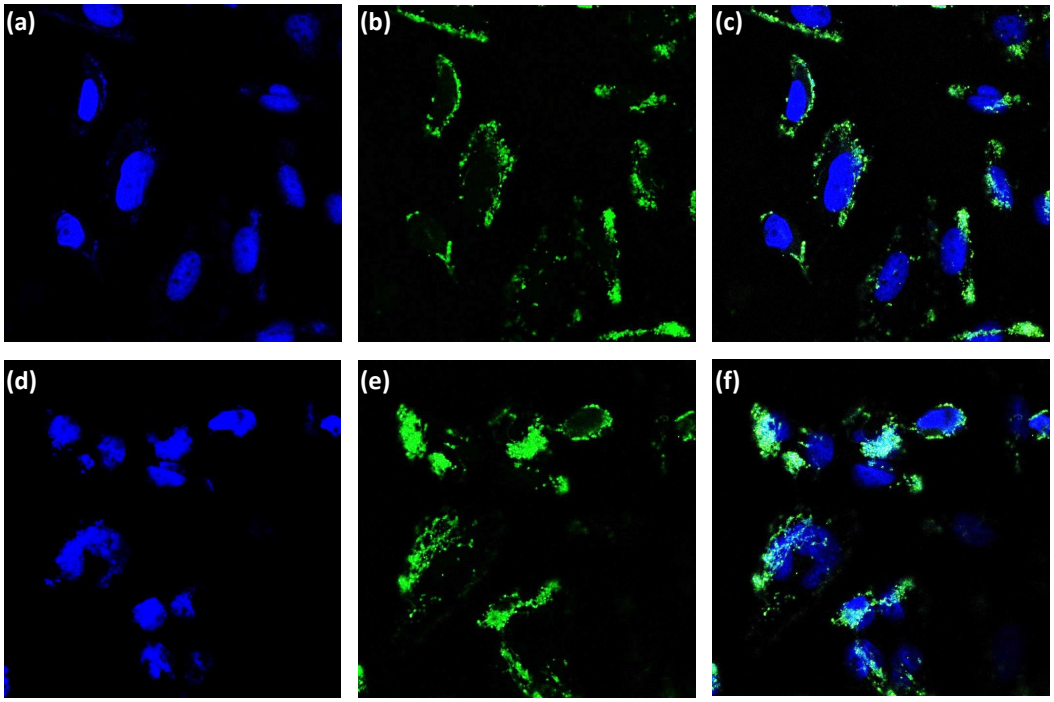

Figure S14.- Confocal microscopy images of live LN229 cells treated with **Lip** (a, b and c) and **Lip+Apt** (d, e and f). LN229 cells were treated with the liposomal formulations at 37°C for 1 hour, after which they were incubated with Hoechst 33342 at 37°C for 30 minutes. Blue nuclear stain, DAPI filter (a and d), green stain (b and e) and merge both channels (c and f).

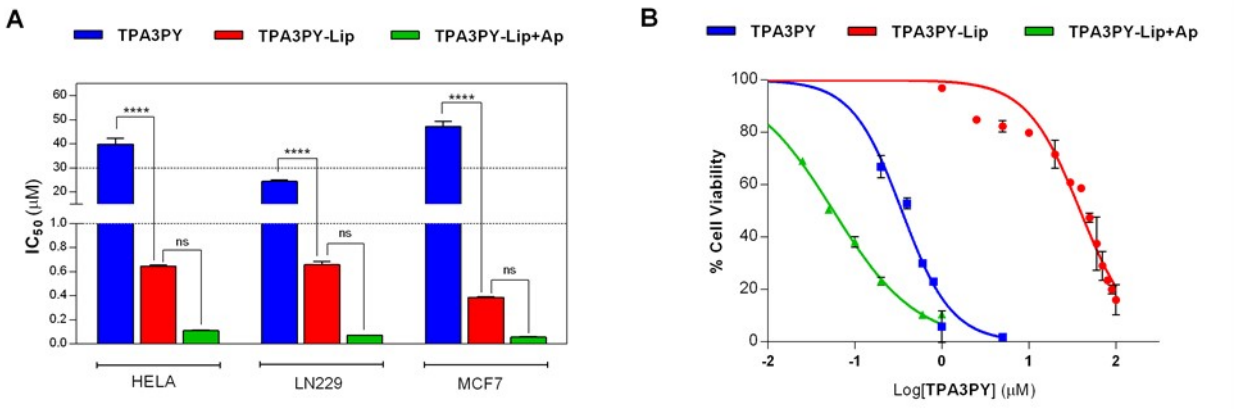

Figure S15.- (a) Values of viability assays (IC_{50}, μM) of the **TPA3Py**, **TPA3Py-Lip** and **TPA3Py-Lip+Apt** systems. (b) Curves of dose-response of **TPA3Py**, **TPA3Py-Lip** and **TPA3Py-Lip+Apt** systems for MCF-7 cancer cell line. Data are expressed as mean ± SD (n=3 independent assays).

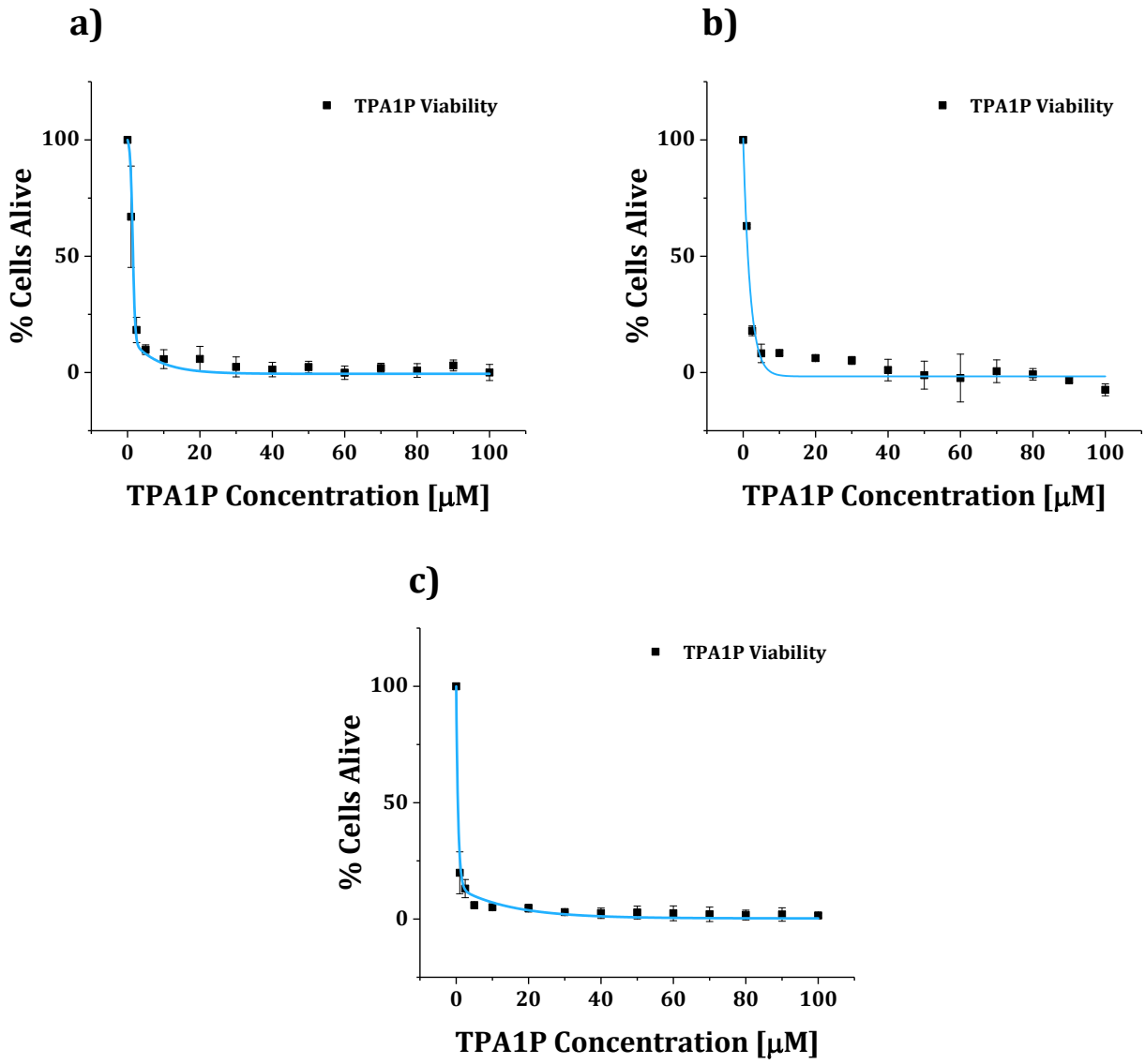

Figure S16.- Curves of dose-response of **TPA1P** for (a) LN229, (b) MCF-7 and (c) HeLa cancer cell lines. Data are expressed as mean ± SD (n=3 independent assays).

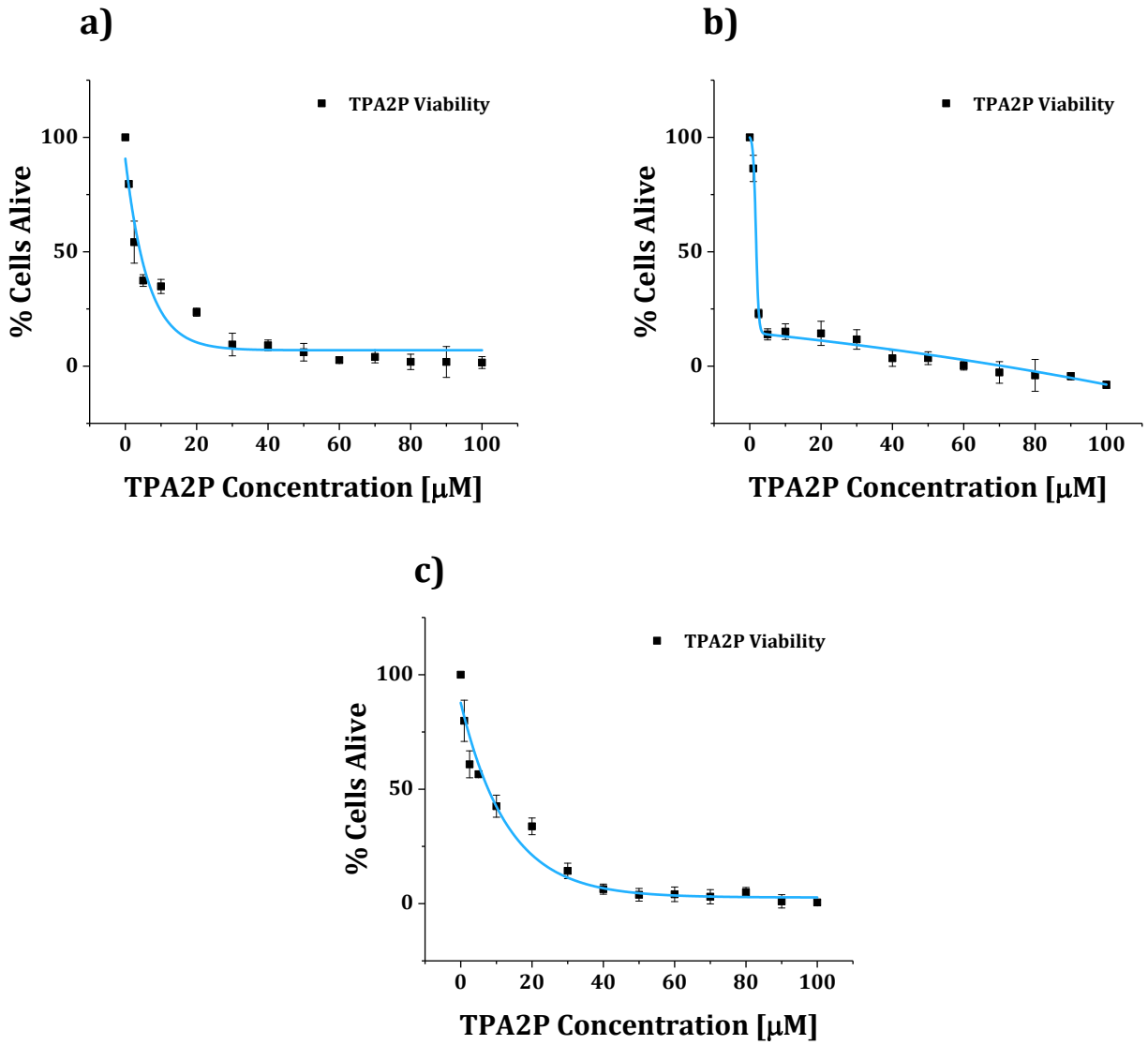

Figure S17.- Curves of dose-response of **TPA2P** for (a) LN229, (b) MCF-7 and (c) HeLa cancer cell lines. Data are expressed as mean ± SD (n=3 independent assays).

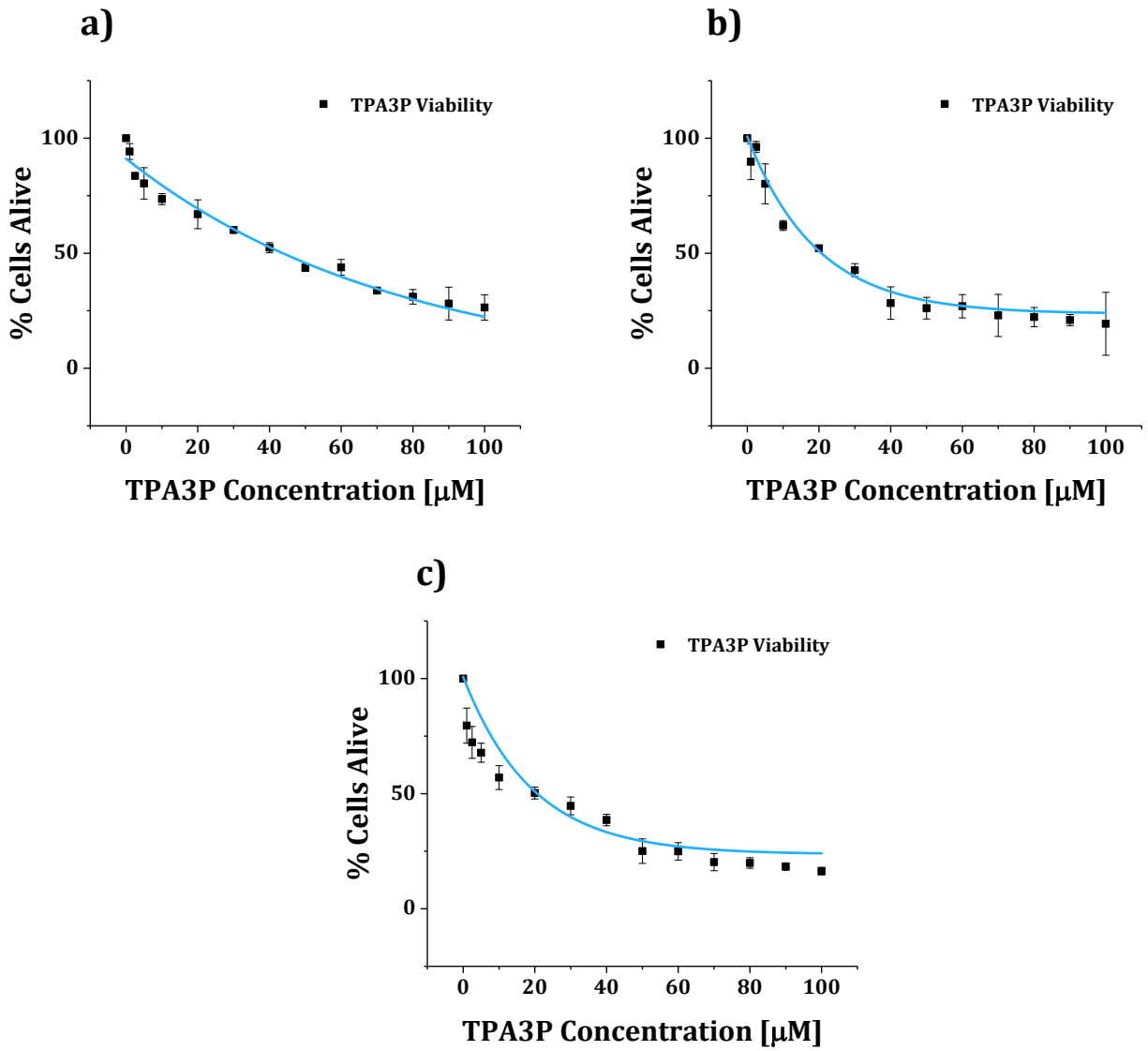

Figure S18.- Curves of dose-response of **TPA3P** for (a) LN229, (b) MCF-7 and (c) HeLa cancer cell lines. Data are expressed as mean ± SD (n=3 independent assays).

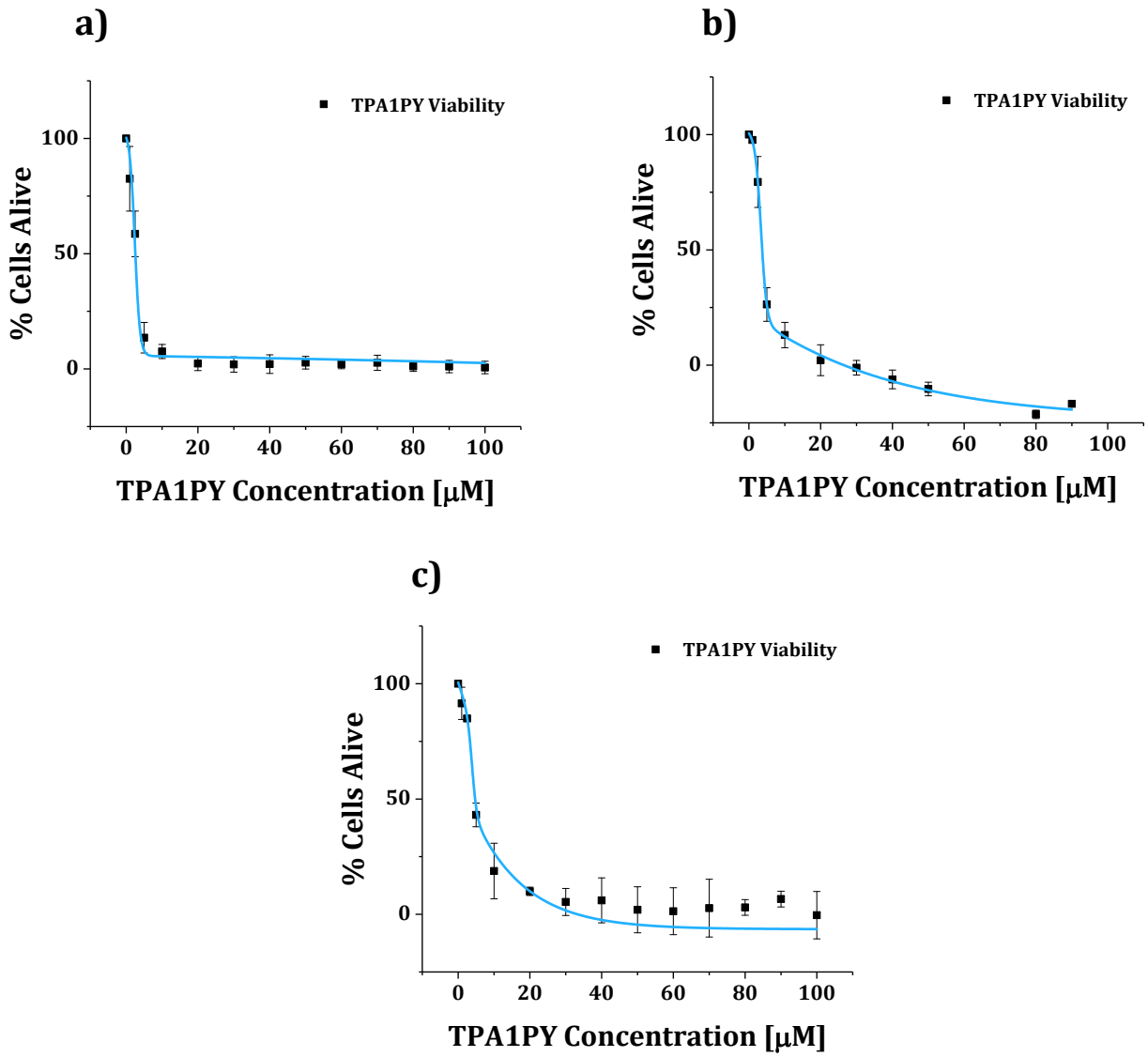

Figure S19.- Curves of dose-response of **TPA1Py** for (a) LN229, (b) MCF-7 and (c) HeLa cancer cell lines. Data are expressed as mean ± SD (n=3 independent assays).

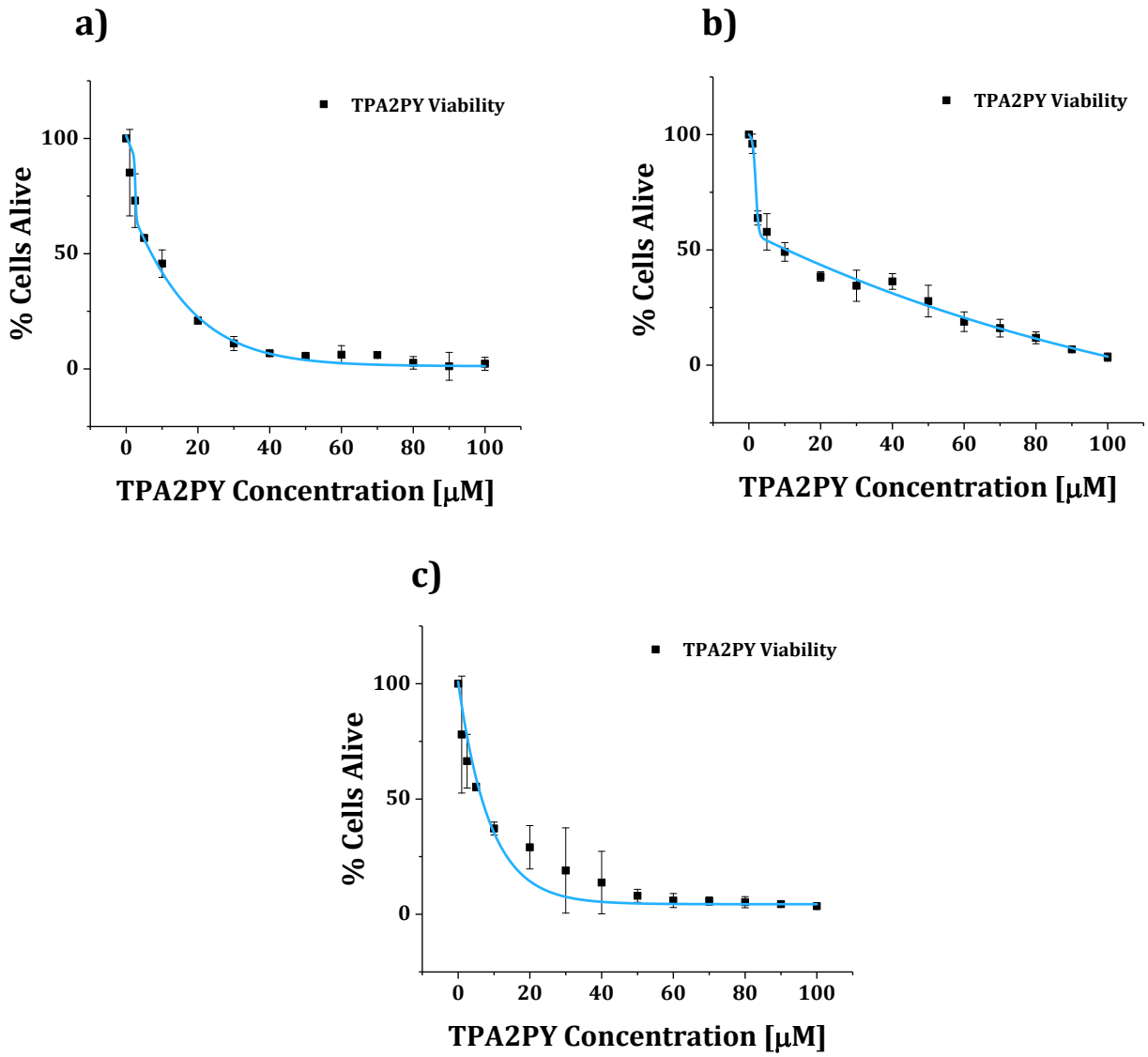

Figure S20.- Curves of dose-response of **TPA2Py** for (a) LN229, (b) MCF-7 and (c) HeLa cancer cell lines. Data are expressed as mean ± SD (n=3 independent assays).

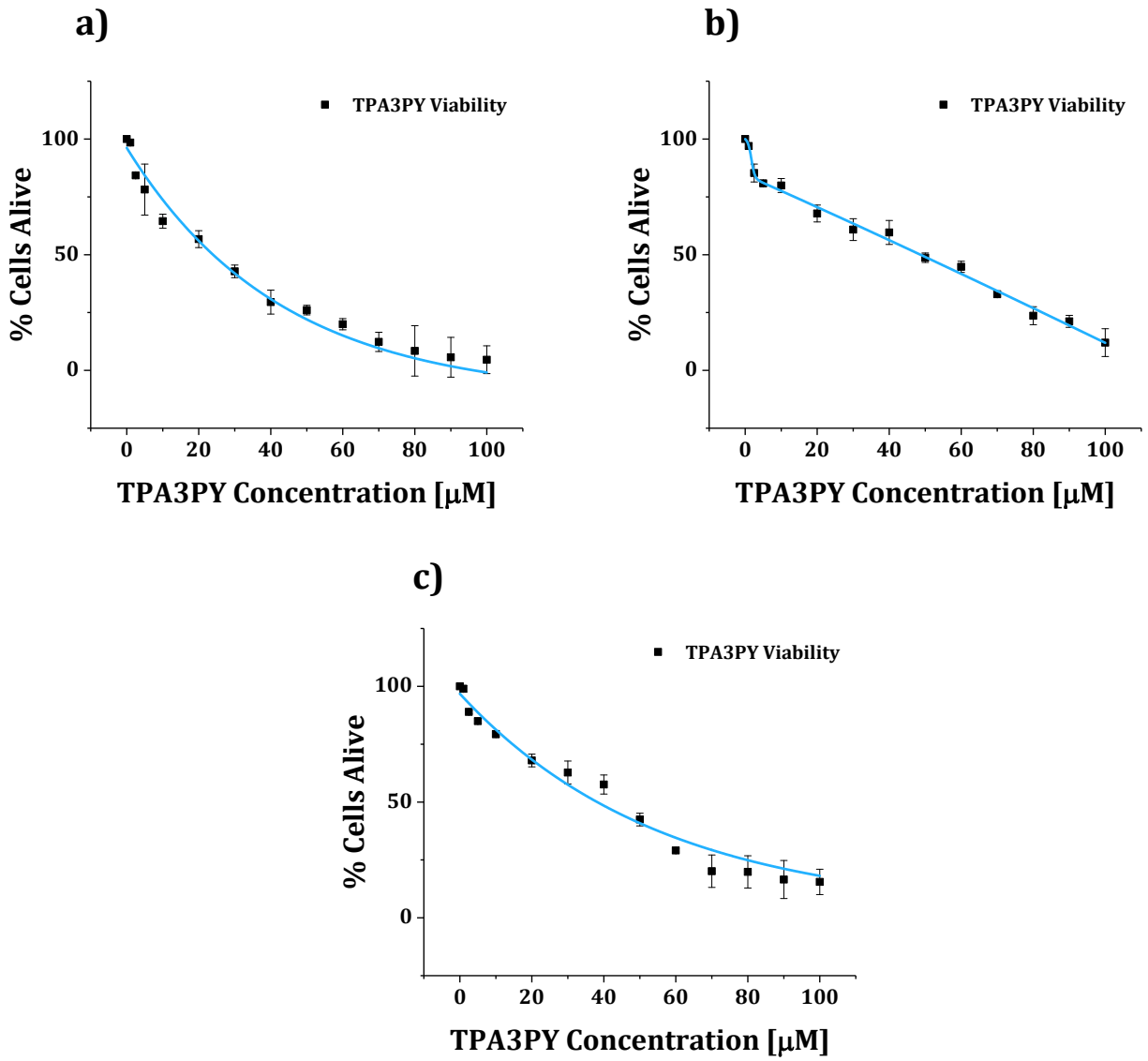

Figure S21.- Curves of dose-response of **TPA3Py** for (a) LN229, (b) MCF-7 and (c) HeLa cancer cell lines. Data are expressed as mean ± SD (n=3 independent assays).

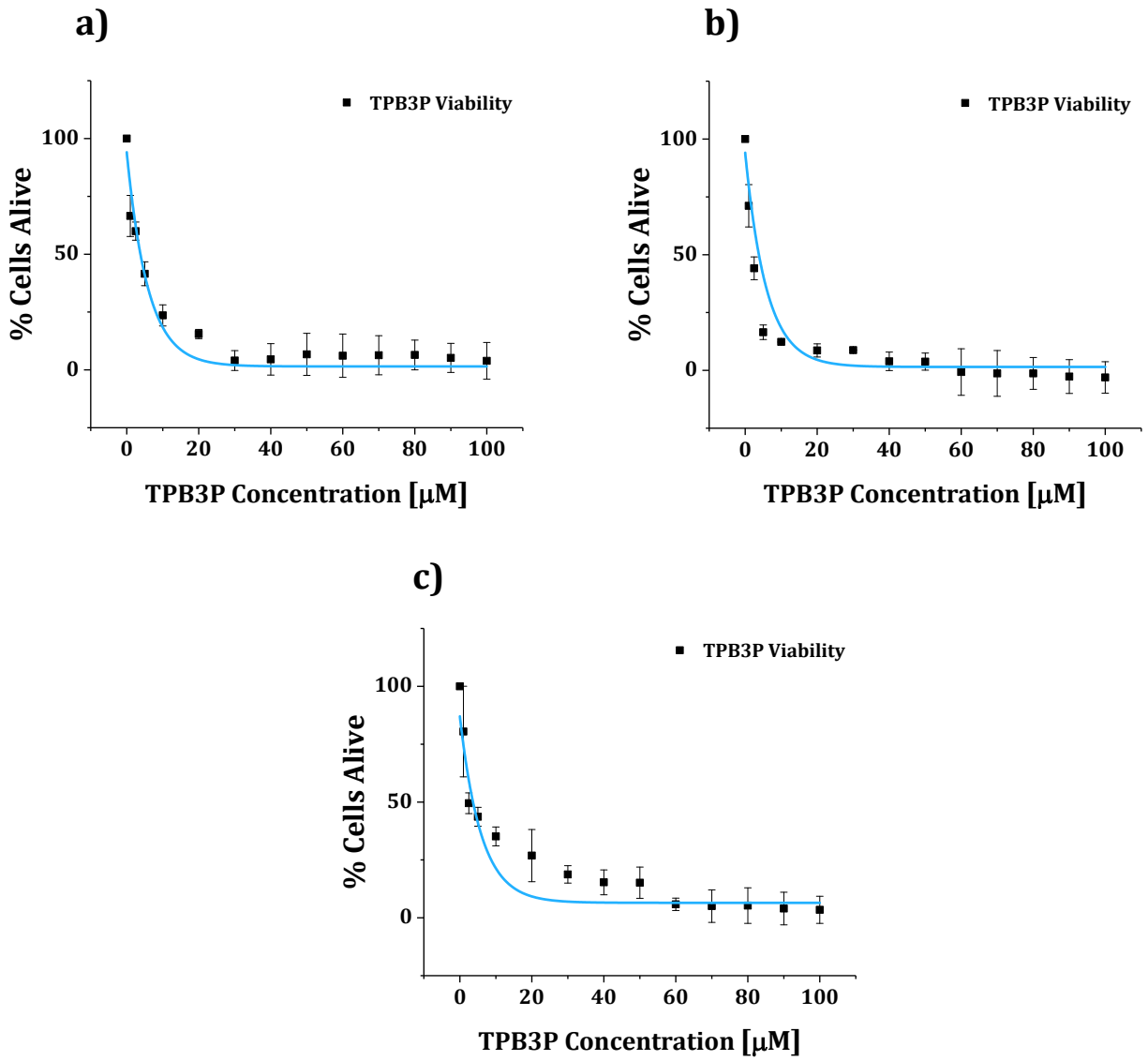

Figure S22.- Curves of dose-response of **TPB3P** for (a) LN229, (b) MCF-7 and (c) HeLa cancer cell lines. Data are expressed as mean ± SD (n=3 independent assays).

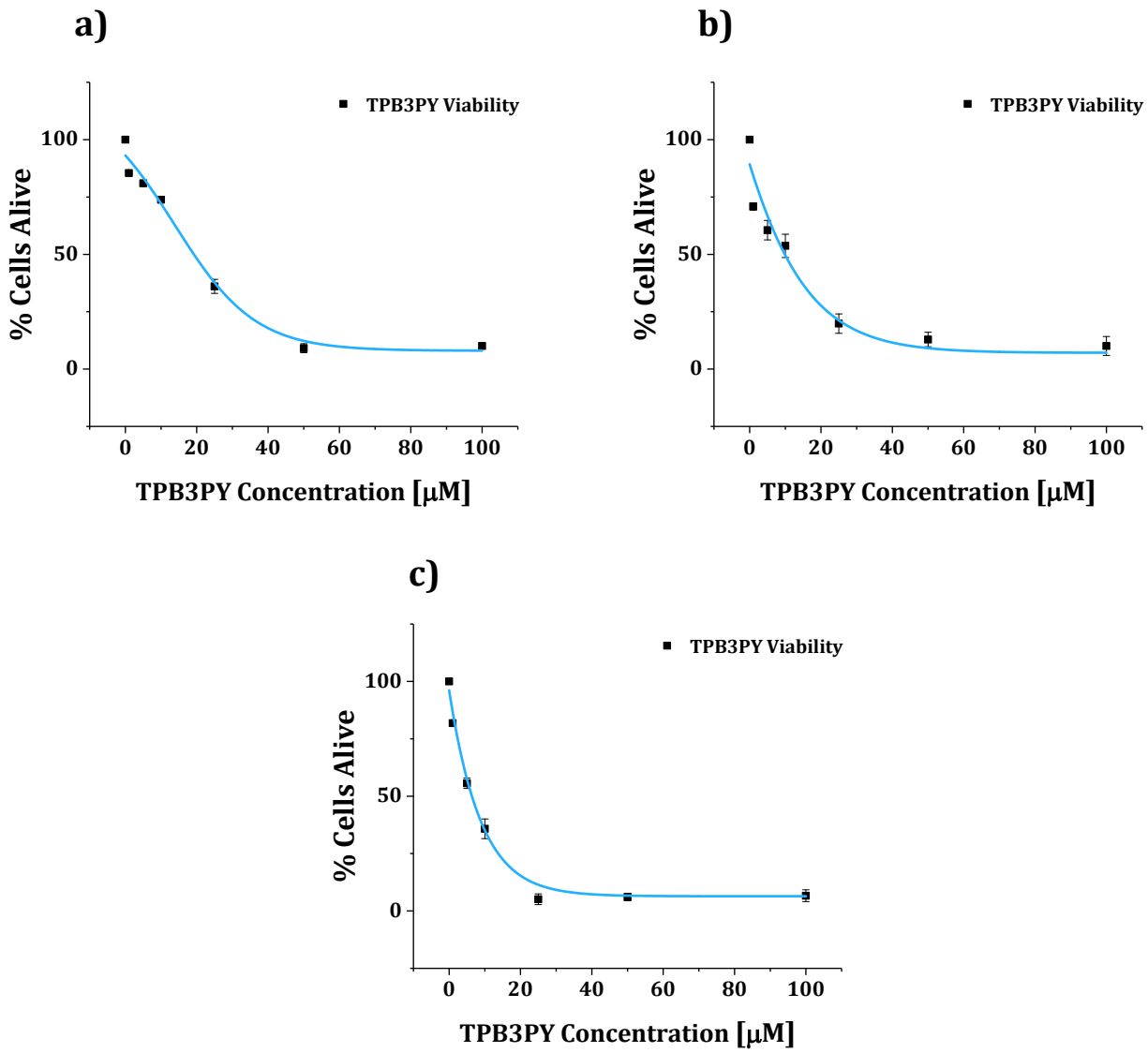

Figure S23.- Curves of dose-response of **TPB3Py** for (a) LN229, (b) MCF-7 and (c) HeLa cancer cell lines. Data are expressed as mean ± SD (n=3 independent assays).

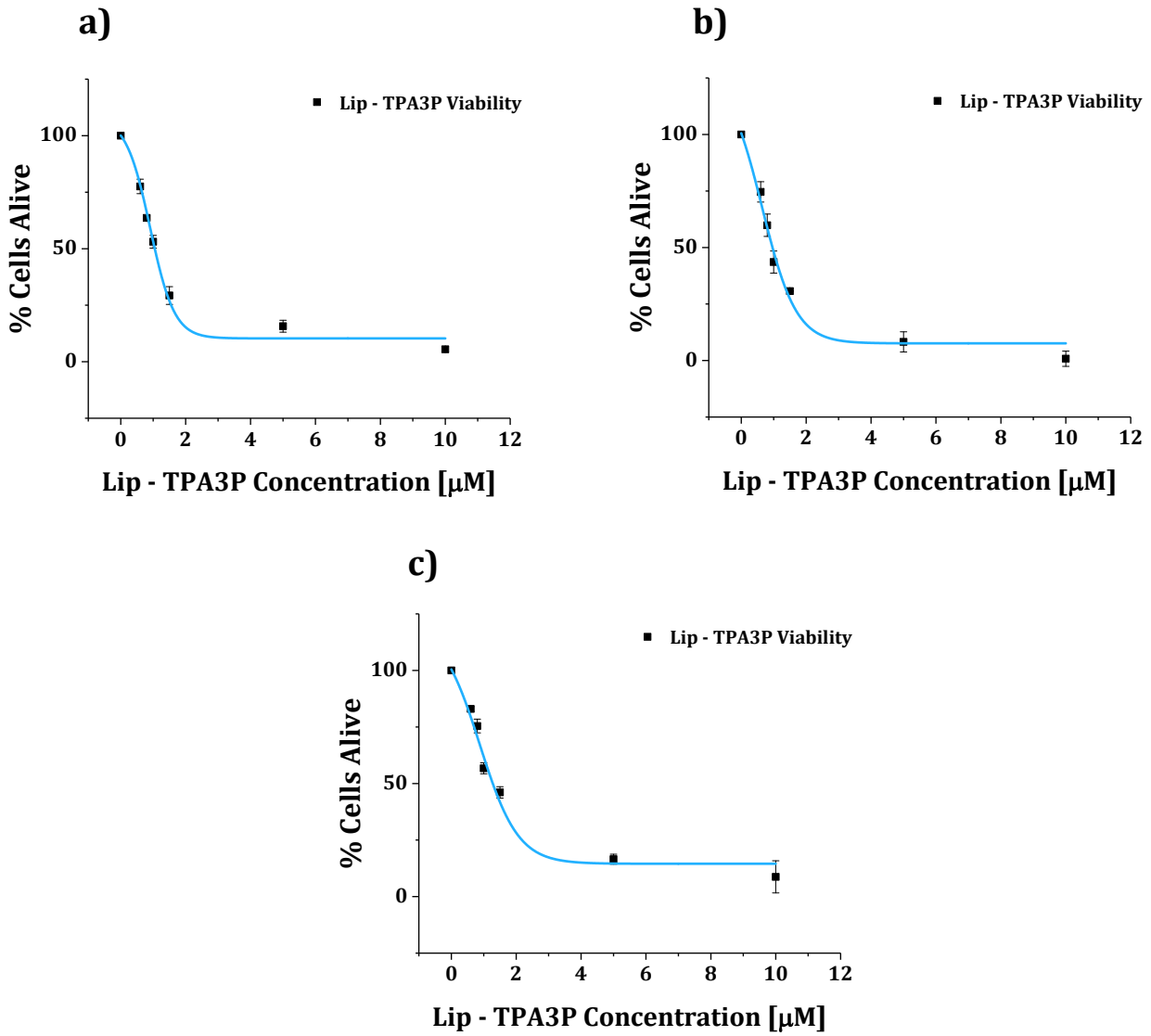

Figure S24.- Curves of dose-response of **TPA3P-Lip** for (a) LN229, (b) MCF-7 and (c) HeLa cancer cell lines. Data are expressed as mean ± SD (n=3 independent assays).

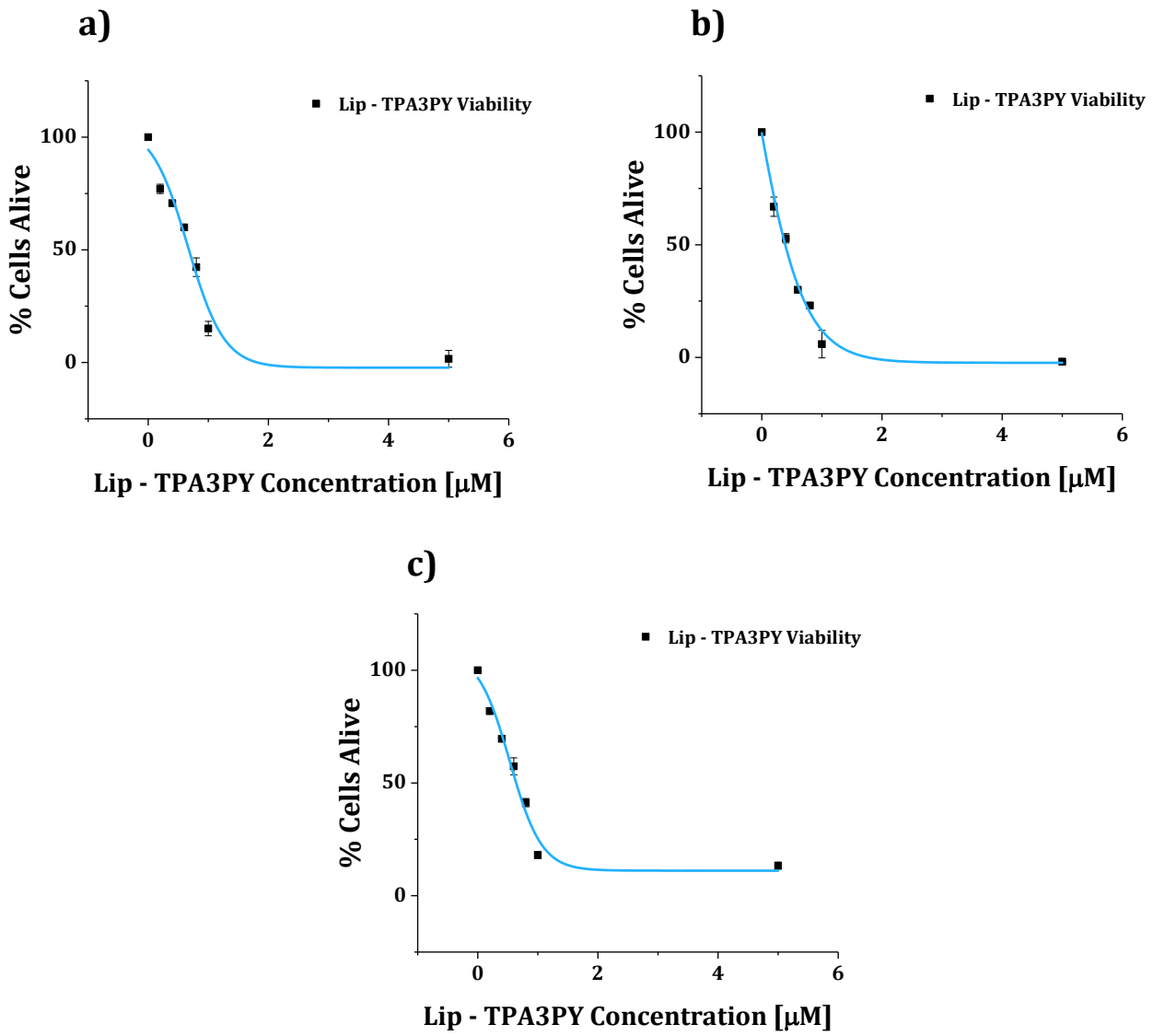

Figure S25.- Curves of dose-response of **TPA3Py-Lip** for (a) LN229, (b) MCF-7 and (c) HeLa cancer cell lines. Data are expressed as mean ± SD (n=3 independent assays).

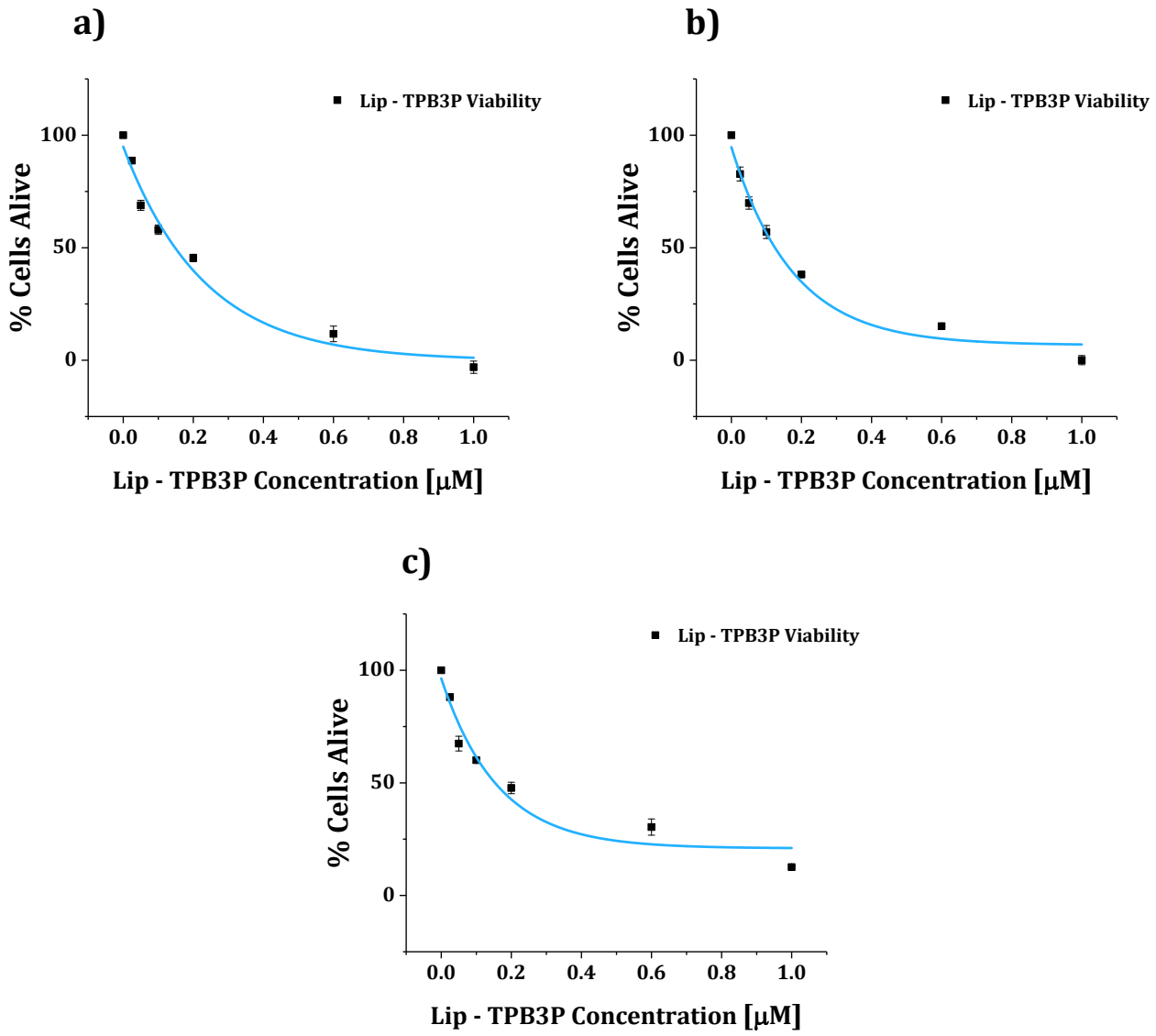

Figure S26.- Curves of dose-response of **TPB3P-Lip** for (a) LN229, (b) MCF-7 and (c) HeLa cancer cell lines. Data are expressed as mean ± SD (n=3 independent assays).

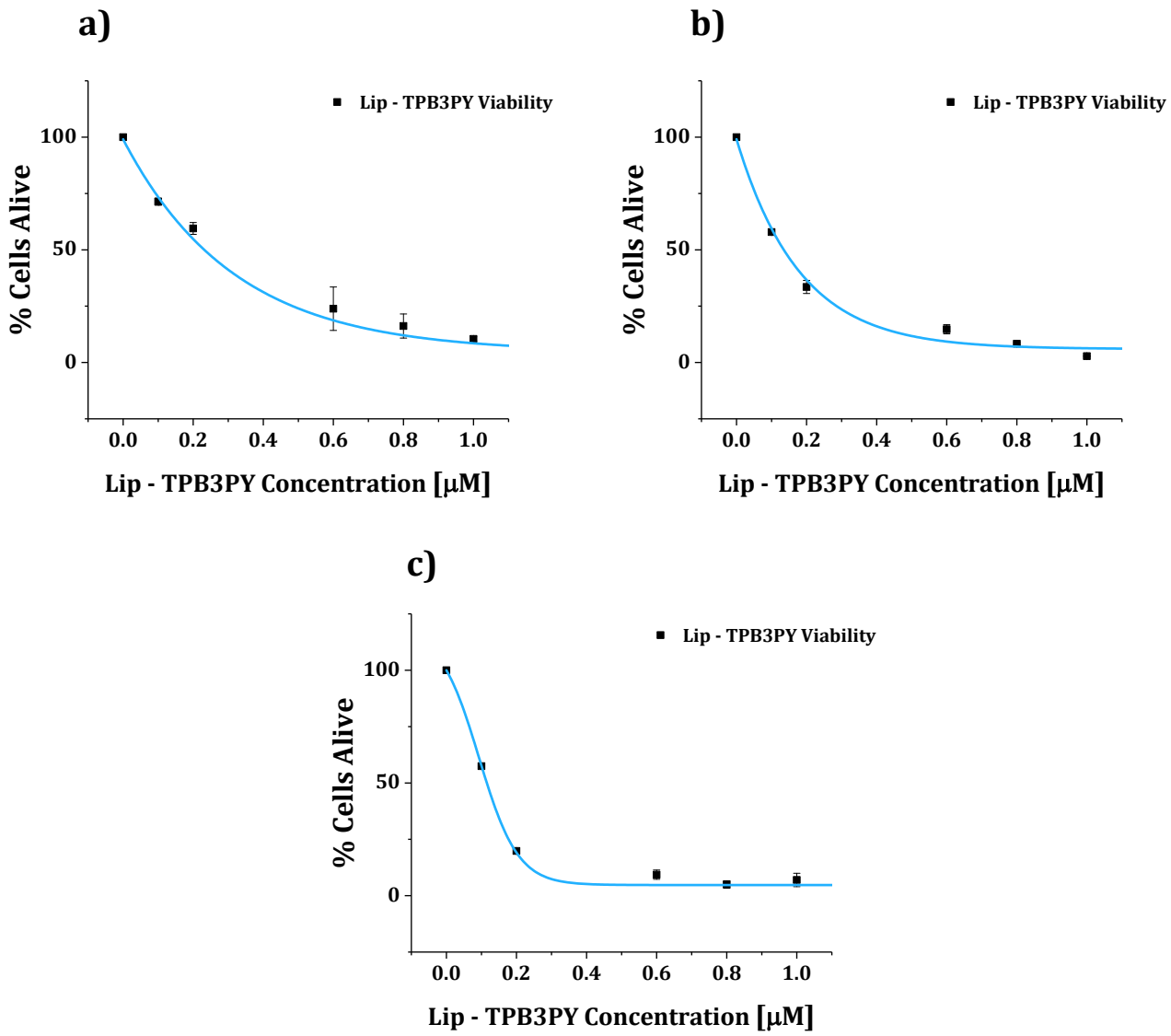

Figure S27.- Curves of dose-response of **TPB3Py-Lip** for (a) LN229, (b) MCF-7 and (c) HeLa cancer cell lines. Data are expressed as mean ± SD (n=3 independent assays).

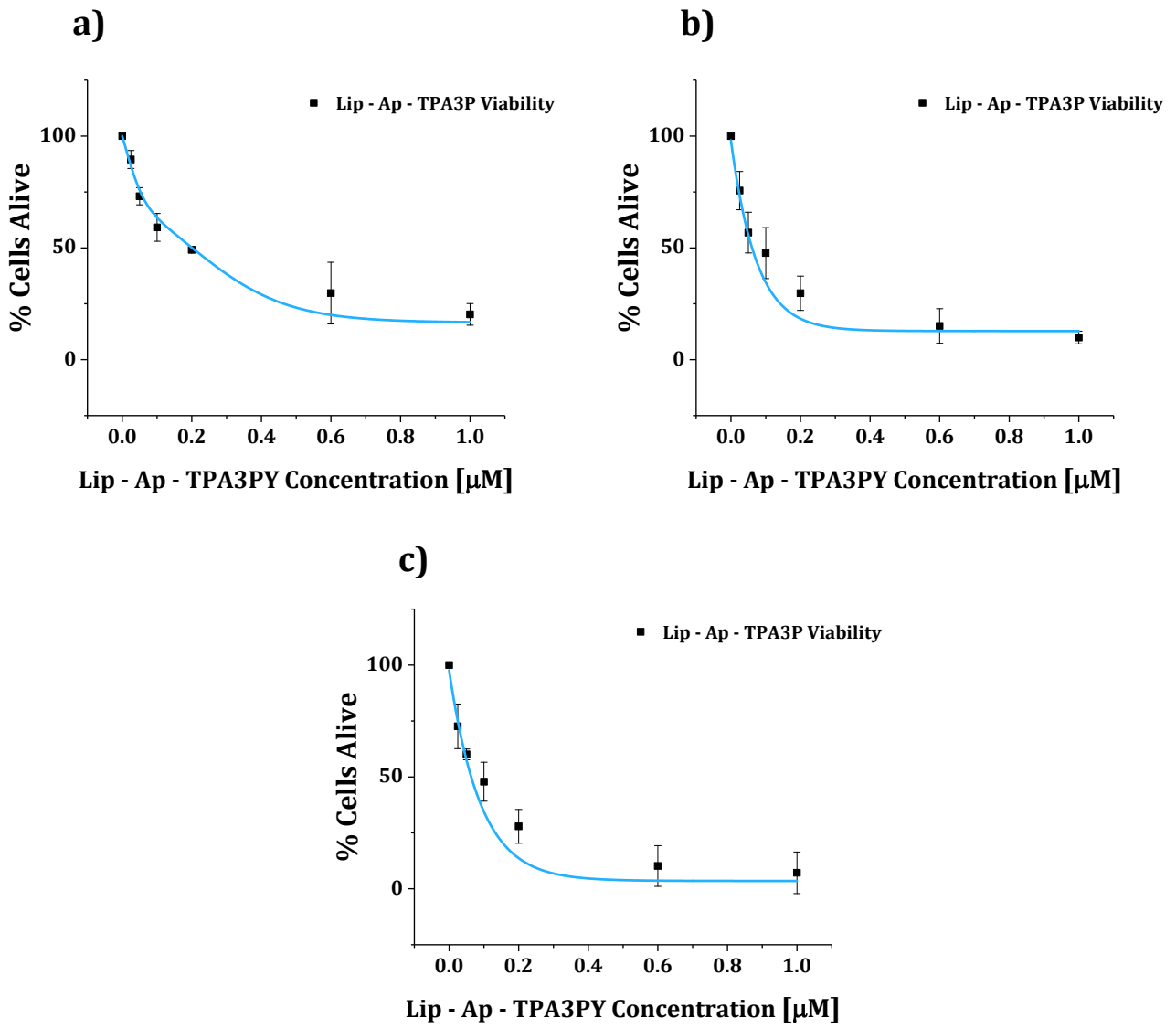

Figure S28.- Curves of dose-response of **TPA3P-Lip-Apt** for (a) LN229, (b) MCF-7 and (c) HeLa cancer cell lines. Data are expressed as mean ± SD (n=3 independent assays).

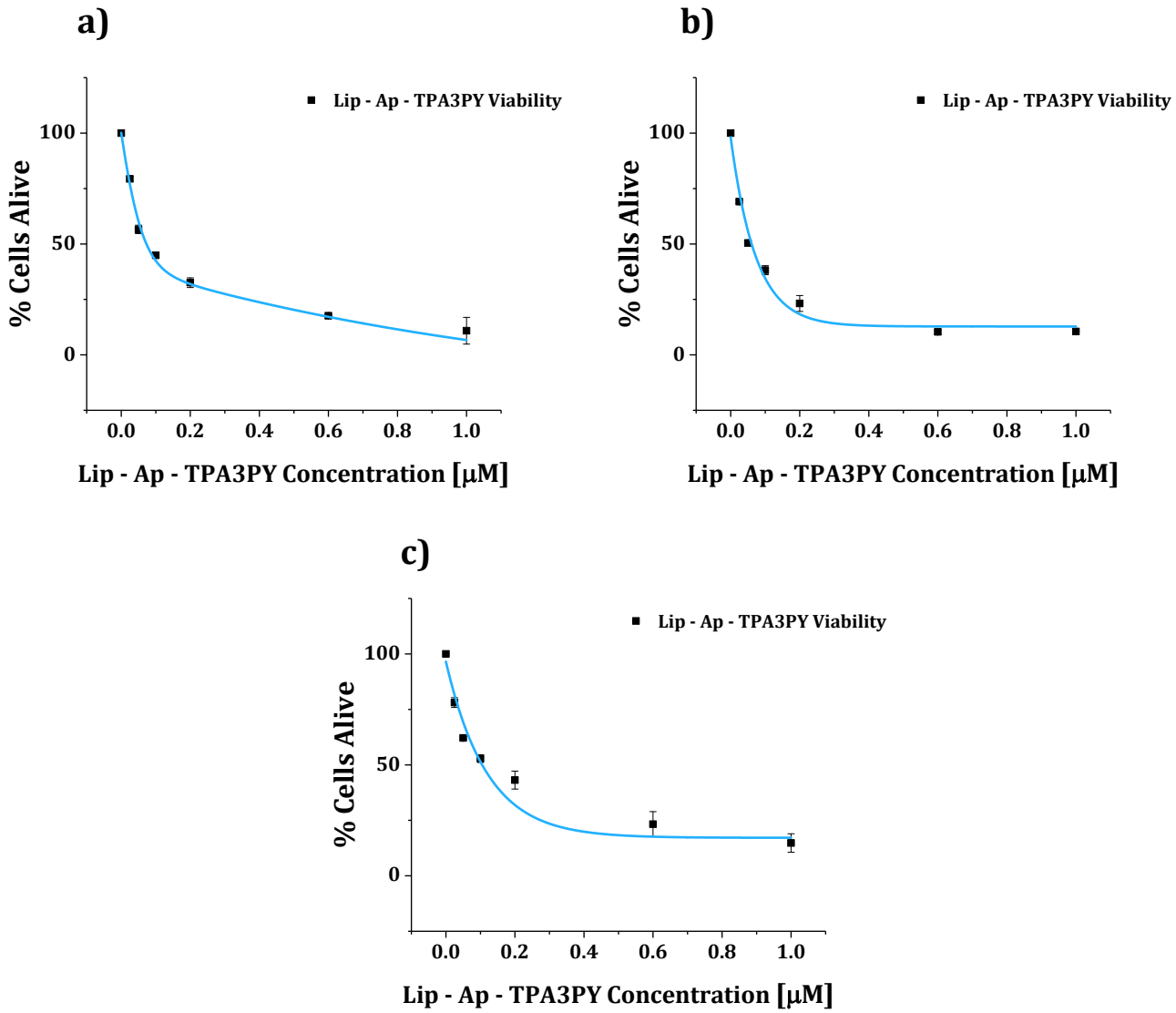

Figure S29.- Curves of dose-response of **TPA3Py-Lip-Apt** for (a) LN229, (b) MCF-7 and (c) HeLa cancer cell lines. Data are expressed as mean ± SD (n=3 independent assays).

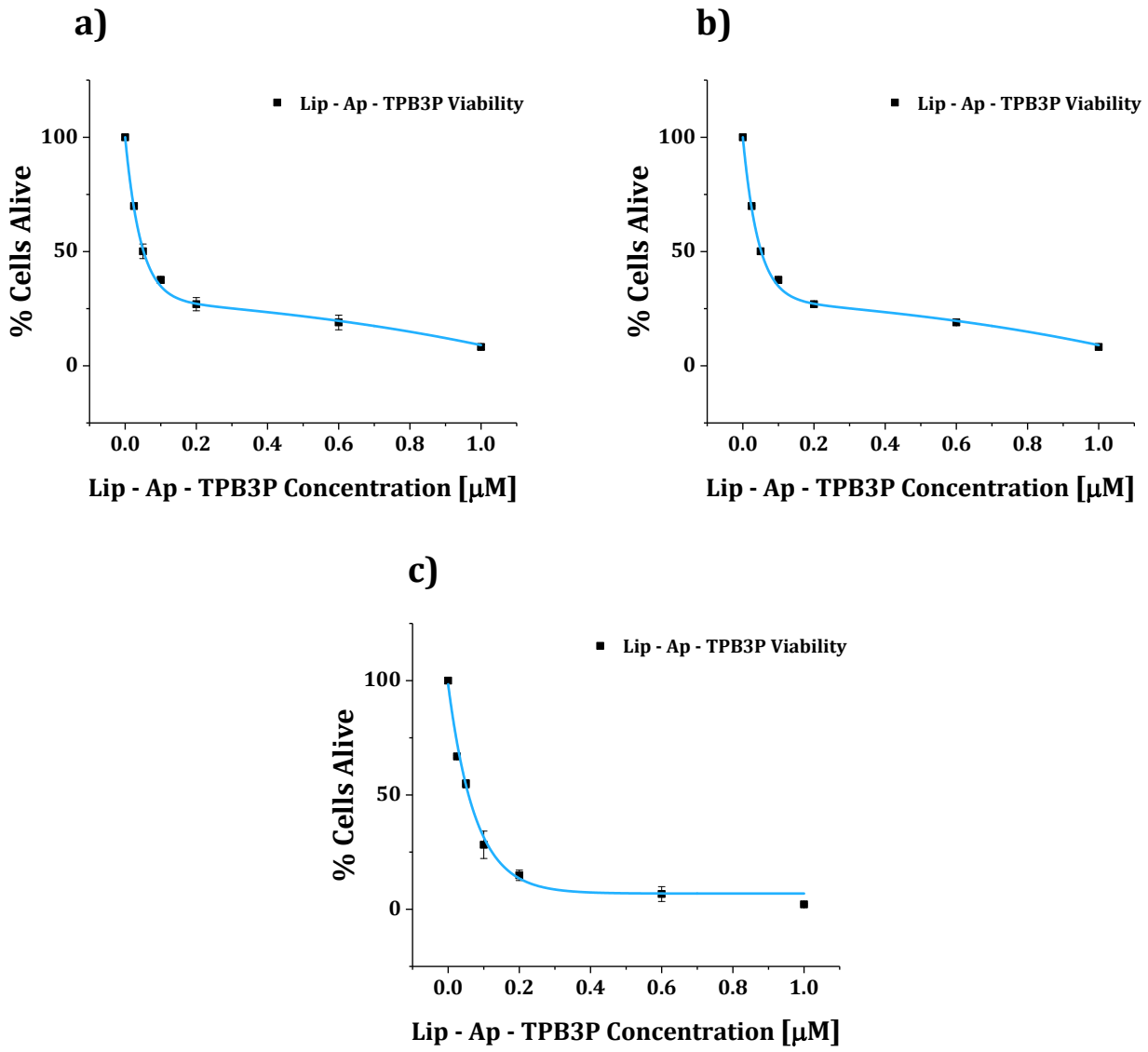

Figure S30.- Curves of dose-response of **TPB3P-Lip-Apt** for (a) LN229, (b) MCF-7 and (c) HeLa cancer cell lines. Data are expressed as mean ± SD (n=3 independent assays).

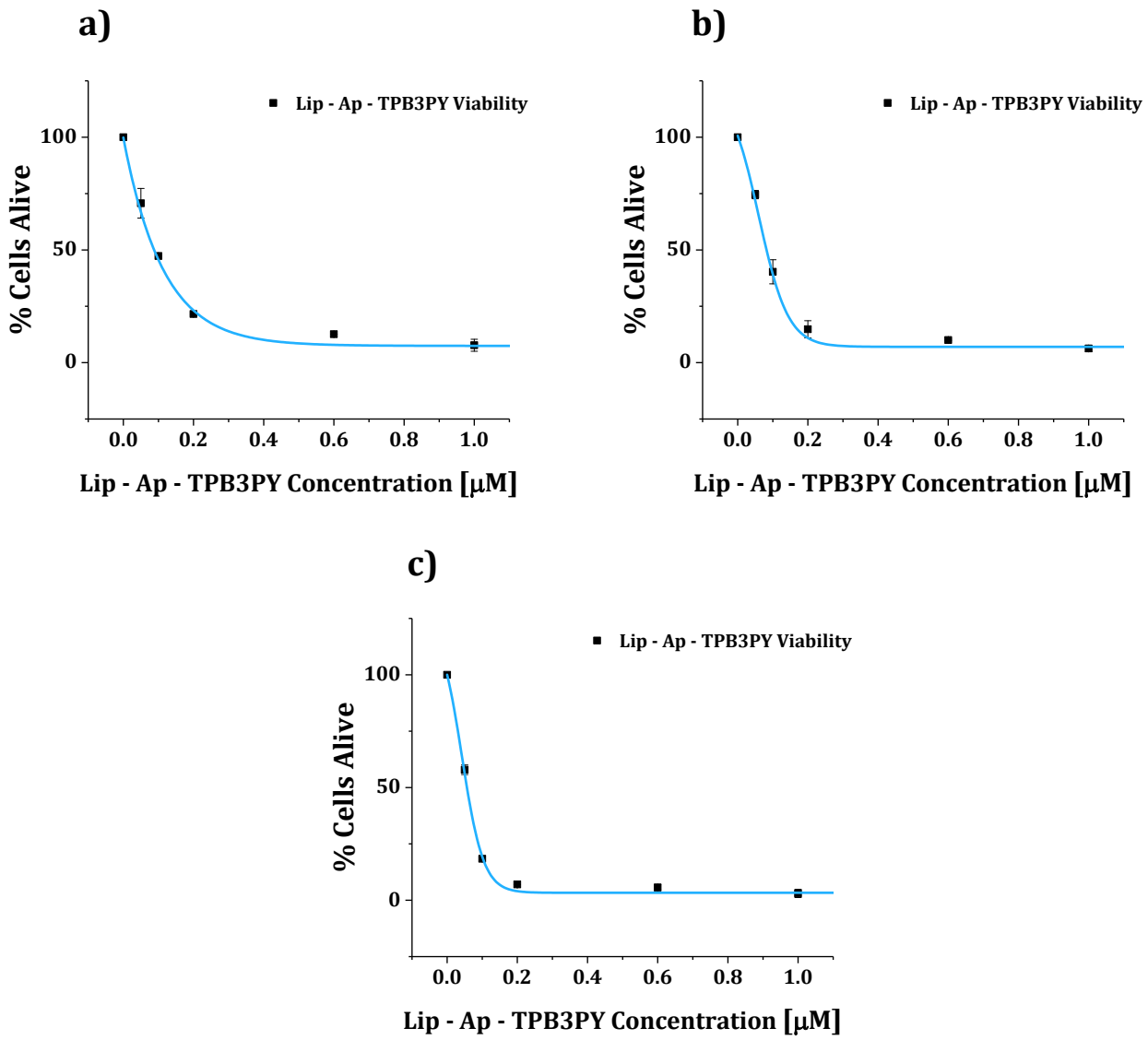

Figure S31.- Curves of dose-response of **TPB3Py-Lip-Apt** for (a) LN229, (b) MCF-7 and (c) HeLa cancer cell lines. Data are expressed as mean ± SD (n=3 independent assays).

3.- References

[1] (a) I. Pont, A. Martínez-Camarena, C. Galiana-Roselló, R. Tejero, M. T. Albelda, J. González-García, R. Vilar and E. García-España, *ChemBioChem*, 2020, **21**, 1167–1177. (b) I. Pont, J. González-García, M. Inclán, M. Reynolds, E. Delgado-Pinar, M. T. Albelda, R. Vilar and E. Garcia-España, *Chem. Eur. J.*, 2018, **24**, 10850–10858.

[2] K. Kimpe, T. N. Parac-Vogt, S. Laurent, C. Piérart, L. V. Elst, R. N. Muller, K. Binnemans, *Eur. J. Inorg. Chem.* 2003, 3021–3027.

[3] T. Mosmann, *J. Immunol. Methods* 1983, **65**, 55–63.